Heavy fermion nondecoupling effects in triple gauge boson vertices

Athanasios Dedes* and Kristaq Suxho†

Division of Theoretical Physics, Physics Department, University of Ioannina, GR 45110, Greece

(Received 27 February 2012; published 29 May 2012)

Within a spontaneously broken gauge group we carefully analyze and calculate triple gauge boson vertices dominated by triangle one-loop Feynman diagrams involving heavy fermions compared to external momenta and gauge boson masses. We perform our calculation strictly in four dimensions and derive a general formula for the off-shell, one-particle irreducible (1PI) effective vertex which satisfies the relevant Ward Identities and the Goldstone boson equivalence theorem. Our goal is to search for nondecoupling heavy fermion effects highlighting their synergy with gauge chiral anomalies. Particularly in the standard model, we find that when the arbitrary anomaly parameters are fixed by gauge invariance and/or Bose symmetry, the heavy fermion contribution cancels its anomaly contribution leaving behind anomaly and mass independent contributions from the light fermions. We apply these results in calculating the corresponding *CP*-invariant one-loop induced corrections to triple gauge boson vertices in the SM, minimal Z' models as well as their extensions with a fourth fermion generation, and compare with experimental data.

DOI: 10.1103/PhysRevD.85.095024 PACS numbers: 12.60.Cn, 12.15.Lk, 13.38.Dg

I. INTRODUCTION

In general, the Appelquist-Carazzone [1] theorem states that the effect from a heavy fermion mass m at low energy observables is suppressed by powers of m. However, this theorem does not hold for theories with chiral gauge couplings or large mass splitting within gauge multiplets, a situation known to take place in the minimal Standard Model (SM) of particle physics [2–4]. Failure of the decoupling of a heavy fermion from radiative corrections requires breaking of a local gauge symmetry and, in addition, breaking of a global symmetry by these corrections [5,6].

Another aspect of theories with chiral gauge couplings is the Adler-Bell-Jackiw or chiral anomaly [7–10]. This is the situation where certain classical Ward Identities (WIs) are violated by quantum corrections (for reviews see [11–13]). For a model that is non-anomaly free, anomalous Ward Identities render it nonrenormalizable and nonunitary. This problem shows up in every symmetry breaking stage of the model. In order to cancel chiral anomalies associated with axial (AAA) or vector-axial (VVA) currents in gauge theories, we either need to stick to only by-construction anomaly-free gauge groups, or, to introduce additional chiral femionic fields [14,15].

An energy region of experimental interest corresponds to the case where a fermion mass m is very heavy, $m_Z^2 < s \ll m^2$, so that it cannot be pair-produced at Tevatron, LHC or a future lepton-collider. If this fermion is chiral i.e., it receives its mass from the Higgs mechanism which is also responsible for the gauge boson mass, then the question of the decoupling of this particle would cause a problem in anomaly cancellation and therefore to gauge invariance. This question has been tackled in many papers in the literature most notably by D'Hoker and Farhi in Refs. [16,17]: decoupling of a fermion whose mass is generated by a Yukawa coupling induces an action functional of the Higgs field and gauge boson fields term, analogous to Wess-Zumino-Witten (WZW) term [18,19] in chiral Lagrangian. Then D'Hoker and Farhi showed that the theory without the decoupled fermion but with the WZW term is gauge invariant. Applications of this nondecoupling effect have been utilized in many physics projects from hadronic up to electroweak physics of the SM and beyond; see, for example, Refs. [20–26]. However, to our knowledge, the above conclusion has not been drawn in the broken phase of theories with spontaneous gauge symmetry breaking like the SM. It is after all meaningful to discuss nondecoupling effects *only* in theories where the physical masses appear explicitly.

The problem when discussing decoupling effects or in general physics associated with the fermionic triangle graph is related to the question: *what is the correct result for such a graph?* The answer depends on the physical set-up in which it arises [27]. For example, as we shall show below in the case of SM, gauge invariance and Bose symmetry are enough to set the triple neutral gauge boson vertices finite and well defined. Only then can we reach the conclusions for the theory at the heavy fermion mass limit.

If the SM gauge group is extended by extra $U(1)$'s then anomaly cancellation conditions become more involved. Recently, the authors of Refs. [28,29] noted that such cancellations may occur inside a "cluster" of anomaly-free heavy fermion sector which is not accessible by the current colliders, leaving behind nondecoupling effects in trilinear gauge boson vertices of the extra massive gauge boson Z' and those of the SM $Z'ZZ$, $Z'WW$, $Z'Z\gamma$ that may

*adedes@cc.uoi.gr
†csoutzio@cc.uoi.gr

be observable at low energies. These effects are visible in the energy region where $M_{Z'} \sim gv < \sqrt{s} \ll m \sim \lambda v$. For these nondecoupling effects to occur it is necessary for fermions and gauge bosons to receive mass from the same Higgs boson and there must be a hierarchy between Yukawa and gauge coupling, $\lambda \sim O(1) \gg g$. In this paper we also elaborate on this issue categorising conditions among couplings where such a situation occurs. We then present a few toy-model examples with two or three different external gauge bosons.

We note in passing that, within field theory, mixed anomaly cancellations via 4d Green-Shwartz mechanism have been discussed and analyzed phenomenologically in many papers e.g. [30–35].

Our goal here is to construct a perturbative, gauge invariant one-loop proper effective vertex for three external gauge bosons that incorporates both chiral anomaly ambiguities together with nondecoupling effects induced by heavy fermions in an explicit manner. We would like to apply this effective vertex in order to:

(i) investigate the interplay between chiral anomaly effects and nondecoupling effects of individual particles in trilinear gauge boson vertices in the SM and its extensions,

(ii) categorise all possible models of mixed anomaly cancellations and nondecoupling effects of very heavy fermions that are directly unreachable at the LHC,

(iii) search for phenomenological implications at colliders.

General Lorentz-invariant expressions for three gauge boson vertices have been analyzed in detail in Refs. [36,37]. One-loop corrections in the SM for the VWW, $V = Z$, γ using dimensional regularization were considered in [5] with special emphasis on the nondecoupling effects due to large doublet mass splittings. The first correct calculation for the $Z\gamma\gamma$ vertex was performed in Ref. [38] while for $ZZ\gamma$ in Ref. [39]. Phenomenological studies including expectations for those interactions at hadron and lepton colliders were studied in detail in Refs. [40–43]. Finally, a complete 1PI vertex for three off-shell gauge bosons is a useful tool in analyzing low energy inelastic scattering processes with a photon in the final state. Dark matter scattering off atomic electrons and nuclei mediated by light gauge boson particles is one application among many (see Refs. [44–46]).

The outline of our article is as follows: in Sec. II, we first present the 1PI effective action for the triple gauge boson vertex and then in Sec. III we discuss all possible and general nondecoupling effects from heavy fermions. These two sections are supplemented by three Appendices A, B, and E, which contain all relevant details of our calculation. The generality of 1PI vertex, $\Gamma^{\mu\nu\rho}$, presented in Sec. II, is to some extend a new result. In addition, the discussion of anomaly driven nondecoupling effects given in Sec. III, is also, to the best of our knowledge, a new material. Section IV contains applications of the general vertex in the SM, in minimal Z' models and their extensions with a fourth sequential generation. Special care has been given to the synergy between the chiral anomaly and the nondecoupling contributions in order to clarify relevant issues in the literature. Appendices C and D deal with the evaluation of charged external gauge boson triple vertices and with analytical expressions of various integrals, respectively. Section V concludes with a brief discussion of our findings.

II. THE TRILINEAR GAUGE BOSON VERTEX

In this section we briefly present the main results for the three gauge boson 1PI vertex, $\Gamma^{\mu\nu\rho}$. The details of this calculation are given in Appendices A and B. Furthermore, the behavior of $\Gamma^{\mu\nu\rho}(s)$ at high energies s, and issues on gauge invariance and Goldstone boson equivalence theorem are discussed in the subsequent subsections.

A. The construction of $\Gamma^{\mu\nu\rho}$

The relevant diagrams are depicted in Fig. 1 and their evaluation is developed in Appendix B. What we basically need in order to calculate the diagrams in Fig. 1 is the interaction part of the Lagrangian

$$\mathcal{L}_{\text{int}} \supset e\bar{\Psi}\gamma^{\mu}(\alpha + \beta\gamma_5)\Psi A_{\mu}, \tag{1}$$

where $\Psi(x)$ is a 4-component spinor consisting of a pair of two Dirac fermions coupled chirally to a vector field $A_{\mu}(x)$. Flavour or spinor indices are silently implied. We shall assume a model interaction for Eq. (1) that arises from a spontaneously broken Abelian gauge theory. A toy model as such is described in Appendix A. Then α and β in Eq. (1) are real numbers (in units of e) related to linear combinations of hypercharges [see for instance Eq. (A8)].

The integral representation for this diagram is given in Eq. (B1). By naive power counting this integral is linearly divergent. This means that when we make a shift of integration variable, e.g., $p \to p + a$, the result depends upon the choice of the arbitrary vector a^{μ}. This change is only reflected in the form factors proportional to k_1 and k_2 in Lorentz invariant expansion of $\Gamma^{\mu\nu\rho}$ [see Eq. (2) below].

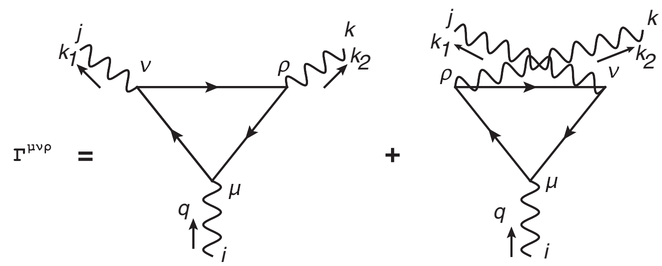

FIG. 1. The one-loop effective trilinear gauge boson vertex, $\Gamma^{\mu\nu\rho}$. The crossed diagram is obtained with the replacement $\{\nu, \rho\} \leftrightarrow \{\rho, \nu\}$ and $k_1 \leftrightarrow k_2$. Indices $\{i, j, k\}$ denote distinct external gauge bosons in general.

As a result, the naive Ward Identities (WIs), Eqs. (B15), (B16), and (B18), are violated by terms that contain the arbitrary four vector a^μ. It is useful to write this four vector as a linear combination of the two independent external momenta: $a^\mu = zk_1^\mu + wk_2^\mu$, with z, w arbitrary real parameters.

In order to write out an explicit form for the trilinear gauge boson vertex, say for three identical massive gauge bosons, we make use of an explicit expression for the triangle graphs first calculated by Rosenberg [38]. The most general form of the axial tensor $\Gamma^{\mu\nu\rho}$, consistent with Lorentz and parity symmetry, is,

$$\Gamma^{\mu\nu\rho}(k_1, k_2; w, z) = [A_1(k_1, k_2; w)\varepsilon^{\mu\nu\rho\sigma}k_{2\sigma} + A_2(k_1, k_2; z)\varepsilon^{\mu\nu\rho\sigma}k_{1\sigma} + A_3(k_1, k_2)\varepsilon^{\mu\rho\beta\delta}k_2^\nu k_{1\beta}k_{2\delta} + A_4(k_1, k_2)\varepsilon^{\mu\rho\beta\delta}k_1^\nu k_{1\beta}k_{2\delta} + A_5(k_1, k_2)\varepsilon^{\mu\nu\beta\delta}k_2^\rho k_{1\beta}k_{2\delta} + A_6(k_1, k_2)\varepsilon^{\mu\nu\beta\delta}k_1^\rho k_{1\beta}k_{2\delta}]. \quad (2)$$

By naive power counting the dimensionless form factors $A_{1,2}$ are infinite. They can be rendered finite by forcing them to obey the relevant, albeit anomalous, Ward Identities. However, $A_{1,2}$ are in general *undetermined* since they depend on arbitrary parameters w and z. This arbitrariness can be fixed by physical requirements like, for example, conservation of charge. On the other hand, the form factors (or integrals) $A_{3\ldots6}$ are finite having dimension of inverse mass square. The latter can be found independently by direct diagrammatic methods. The whole procedure is described in detail in Appendix B.

Therefore, nondecoupling effects should originate solely from the A_1 and A_2 parts of $\Gamma^{\mu\nu\rho}$ but without any further physical input they are undetermined. A direct calculation of $A_{1,2}$ with dimensional regularization [47] or with Pauli-Villars regularization is not a good choice when shifting integration variables within linearly (and above) divergent Feynman integrals in four dimensions [48–50]. The outcome for a single external gauge boson ($i = j = k$ in Fig. 1) triangle graph is appended in Eqs. (B26)–(B28). From these expressions and from Eq. (2) we obtain $A_1(k_1, k_2; w)$ and $A_2(k_1, k_2; z)$ in terms of the finite integrals $A_{3\ldots6}$. The corresponding results, in the case of three external identical gauge bosons, are given by Eqs. (B37) and (B38) while the finite integrals $A_{3\ldots6}$ by Eqs. (B33)–(B35).

Furthermore, although Bose symmetry could constrain the arbitrary numbers w and z, it is not enough to eliminate them altogether: a physical condition is needed, e.g., conservation of electric charge for fermions coupled to external photons or vanishing triangle graph for on-shell momenta of massive gauge bosons or, even, a pure theoretical reason, like the decoupling property.

It is straightforward, albeit tedious, to generalize $\Gamma^{\mu\nu\rho}$ in Eq. (2) to the case of three distinct external, massive or massless, gauge bosons ($i \neq j \neq k$ in Fig. 1). With the assignments depicted in Fig. 1, the generalized Ward Identities for vertices μ, ν, ρ are written, respectively, as[1]

$$q_\mu\Gamma^{\mu\nu\rho}(k_1, k_2, w, z) = im_{A_i}\Gamma^{\nu\rho}(k_1, k_2) + \frac{e^3[(\alpha_i\alpha_j + \beta_i\beta_j)\beta_k + (\alpha_i\beta_j + \alpha_j\beta_i)\alpha_k]}{4\pi^2}\varepsilon^{\lambda\nu\rho\sigma}k_{1\lambda}k_{2\sigma}(w - z), \quad (3a)$$

$$-k_{1\nu}\tilde{\Gamma}^{\nu\rho\mu}(k_1, k_2, w, z) = im_{A_j}\tilde{\Gamma}^{\rho\mu}(k_1, k_2) + \frac{e^3[(\alpha_j\alpha_k + \beta_j\beta_k)\beta_i + (\alpha_j\beta_k + \alpha_k\beta_j)\alpha_i]}{4\pi^2}\varepsilon^{\lambda\mu\rho\sigma}k_{1\lambda}k_{2\sigma}(w - 1), \quad (3b)$$

$$-k_{2\rho}\hat{\Gamma}^{\rho\mu\nu}(k_1, k_2, w, z) = im_{A_k}\hat{\Gamma}^{\mu\nu}(k_1, k_2) + \frac{e^3[(\alpha_k\alpha_i + \beta_k\beta_i)\beta_j + (\alpha_k\beta_i + \alpha_i\beta_k)\alpha_j]}{4\pi^2}\varepsilon^{\lambda\mu\nu\sigma}k_{1\lambda}k_{2\sigma}(z + 1), \quad (3c)$$

where the corresponding Γ, $\tilde{\Gamma}$, and $\hat{\Gamma}$ are appended in Eqs. (B47) and (B48). It is remarkable here to note the i'th gauge boson mass, $m_{A_i} = -2\beta_i ev$, in front of the pseudoscalar 1PI function $\Gamma^{\nu\rho}$. This term and the analogous in Eqs. (3b) and (3c) are the source of heavy fermion mass nondecoupling effects since in the formal limit of $m \to \infty$ there is a remaining piece of order $e^3\varepsilon^{\lambda\nu\rho\sigma}k_{1\lambda}k_{2\sigma}/4\pi^2$ in $\Gamma^{\mu\nu\rho}$ for example. On the other hand, it shows that currents which are associated to unbroken symmetry generators i.e., to massless gauge bosons, do not provide any nondecoupling effect in $\Gamma^{\mu\nu\rho}$. Moreover, $\Gamma^{\nu\rho}$, $\tilde{\Gamma}^{\rho\mu}$, $\hat{\Gamma}^{\mu\nu}$ depend linearly upon the Yukawa coupling λ, that is responsible for the fermion mass through the Higgs mechanism and vanishes in the limit of $\lambda \to 0$.[2]

Using the WI's for the vertices ν and ρ, i.e., Eqs. (3b) and (3c) as well as Eq. (2), we obtain the following expressions for the integrals A_1 and A_2:

[1]In order not to clutter the notation we suppress indices i, j, k in the following expressions for Γ's.
[2]Throughout, we assume chiral fermions that receive mass through Yukawa interactions with the Higgs field.

$$A_1(k_1, k_2; w) = (k_1 \cdot k_2)A_3 + k_1^2 A_4 - \frac{e^3 m^2 \beta_j}{\pi^2} I_1(k_1, k_2, m) + \frac{e^3[(\alpha_j\alpha_k + \beta_j\beta_k)\beta_i + (\alpha_j\beta_k + \alpha_k\beta_j)\alpha_i]}{4\pi^2}(w-1), \tag{4a}$$

$$A_2(k_1, k_2; z) = (k_1 \cdot k_2)A_6 + k_2^2 A_5 - \frac{e^3 m^2 \beta_k}{\pi^2} I_2(k_1, k_2, m) + \frac{e^3[(\alpha_i\alpha_k + \beta_i\beta_k)\beta_j + (\alpha_i\beta_k + \alpha_k\beta_i)\alpha_j]}{4\pi^2}(z+1), \tag{4b}$$

where the ''nondecoupled'' integrals are given by

$$I_1(k_1, k_2, m) = \int_0^1 dx \int_0^{1-x} dy \frac{-(\alpha_i\alpha_k + \beta_k\beta_i) + 2x\beta_i\beta_k}{\Delta}, \tag{5a}$$

$$I_2(k_1, k_2, m) = \int_0^1 dx \int_0^{1-x} dy \frac{(\alpha_i\alpha_j + \beta_i\beta_j) - 2y\beta_i\beta_j}{\Delta}, \tag{5b}$$

with

$$\begin{aligned}\Delta &\equiv \Delta(k_1, k_2) \\ &= x(x-1)k_2^2 + y(y-1)k_1^2 - 2xyk_1 \cdot k_2 + m^2.\end{aligned} \tag{6}$$

The following limits,

$$\lim_{m\to\infty} m^2 I_1(k_1, k_2, m) = -\frac{1}{6}(3\alpha_i\alpha_k + \beta_i\beta_k), \tag{7a}$$

$$\lim_{m\to\infty} m^2 I_2(k_1, k_2, m) = \frac{1}{6}(3\alpha_i\alpha_j + \beta_i\beta_j), \tag{7b}$$

are also useful in simplifying formulae when discussing synergies of anomalous and nondecoupling terms.

We are now ready to complete $\Gamma^{\mu\nu\rho}$ in Eq. (2) by reading directly from Eq. (B47) the finite (in four dimensions) terms $A_{3\ldots6}$. We find:

$$A_3(k_1, k_2) = -\frac{e^3[(\alpha_i\alpha_j + \beta_i\beta_j)\beta_k + (\alpha_i\beta_j + \beta_i\alpha_j)\alpha_k]}{\pi^2} \int_0^1 dx \int_0^{1-x} dy \frac{xy}{\Delta}, \tag{8a}$$

$$A_4(k_1, k_2) = \frac{e^3[(\alpha_i\alpha_j + \beta_i\beta_j)\beta_k + (\alpha_i\beta_j + \beta_i\alpha_j)\alpha_k]}{\pi^2} \int_0^1 dx \int_0^{1-x} dy \frac{y(y-1)}{\Delta}, \tag{8b}$$

$$A_5(k_1, k_2) = -\frac{e^3[(\alpha_i\alpha_j + \beta_i\beta_j)\beta_k + (\alpha_i\beta_j + \beta_i\alpha_j)\alpha_k]}{\pi^2} \int_0^1 dx \int_0^{1-x} dy \frac{x(x-1)}{\Delta}, \tag{8c}$$

$$A_6(k_1, k_2) = -A_3(k_1, k_2). \tag{8d}$$

One could guess the expressions above with $i \neq j \neq k$ from the ones with a single identical gauge boson $i = j = k$ by exploiting simple combinatoric algebra in Eqs. (B33)–(B35), (B37), and (B38). One can check that all the above form factors obey the Bose symmetry specified in Eqs. (B39a)–(B39c).

In summary, our main result is the trilinear gauge boson vertex $\Gamma^{\mu\nu\rho}$ of Eq. (2), supplemented by form factor components $A_{i=1\ldots6}$ read from Eqs. (4) and (8). Equation (2) satisfies the relevant Ward Identities stated in Eq. (3) which originate from the partial conservation of vector and axial vector symmetries in (A9).

B. Unitarity

We can make full use of the effective vertex $\Gamma^{\mu\nu\rho}$ in order to calculate, as an example, the matrix element for the process $ZZ \to ZZ$ with an intermediate massive vector boson Z'. We perform the calculation in the center of mass frame with the following kinematics:

$$\begin{aligned} p_1 &= (E, 0, 0, p), \qquad p_2 = (E, 0, 0, -p), \\ k_1 &= (E, p\sin\theta, 0, p\cos\theta), \\ k_2 &= (E, -p\sin\theta, 0, -p\cos\theta), \\ \varepsilon(p_1) &= \frac{1}{m_Z}(p, 0, 0, E), \qquad \varepsilon(p_2) = \frac{1}{m_Z}(p, 0, 0, -E), \\ \varepsilon(k_1) &= \frac{1}{m_Z}(p, E\sin\theta, 0, E\cos\theta), \\ \varepsilon(k_2) &= \frac{1}{m_Z}(p, -E\sin\theta, 0, -E\cos\theta), \end{aligned}$$

where p_1 and p_2 are the four-momenta of incoming particles, k_1 and k_2 the four-momenta of outgoing particles, $\varepsilon(p_1)$, $\varepsilon(p_2)$, $\varepsilon(k_1)$, $\varepsilon(k_2)$ are the polarization vectors of the incoming and outgoing particles, respectively, and θ is the scattering angle of the outgoing Z boson in the center of mass frame. Nonzero contributions arise only from t and u-channels since the s-channel amplitude vanishes in this frame. Working in the unitary gauge, we find a contribution to $ZZ \to ZZ$ due to loop-induced $\Gamma^{\mu\nu\rho}_{Z'ZZ}$ of Eq. (2) as,

$$\mathcal{M} = \mathcal{M}_t + \mathcal{M}_u = \left(\frac{E^2\sin^2\theta}{t - m_{Z'}^2}\right)[(A_1 - A_2) + p^2(1 - \cos\theta)(A_3 - A_6)]^2 + \left(\frac{E^2\sin^2\theta}{u - m_{Z'}^2}\right)[(A_1 - A_2) + p^2(1 + \cos\theta)(A_3 - A_6)]^2, \tag{9}$$

where $t = (p_1 - k_1)^2 = -2p^2(1 - \cos\theta)$ and $u = (k_1 - p_2)^2 = -2p^2(1 + \cos\theta)$. The factors A_1 and A_2 in Eq. (4) are dimensionless and, in the limit of $E^2 \to \infty$ vary at worse as constants while from Eq. (8) we have $A_3 = -A_6$ which asymptotically goes like E^{-2}. Therefore at high energies $E^2 \to \infty$, terms inside the square brackets in Eq. (9) behave like constants and so the amplitude does at high energies. This means that unitarity is satisfied as is of course expected for a renormalized theory. It is worthwhile noting that in the limit $E^2 \to \infty$ we obtain $(A_1 - A_2) \propto c(w - z)$, where c is the anomaly prefactor present in the second term in the r.h.s of Eq. (3a). There is still however a finite and nonvanishing constant contribution from the $A_{3,6}$ form factors in Eq. (9) which for every particle contribution reads,

$$\lim_{E^2\to\infty} \mathcal{M} = -\left(\frac{c}{4\pi^2}\right)^2 \sin^2\theta\left[1 + 2(w - z) + \frac{(w - z)^2}{2\sin^2\theta}\right]. \tag{10}$$

We observe that the unknown parameters w and z still remain in the amplitude. Only the relation $w = z$ removes them from the asymptotic limit. We shall come back at this point when discussing the Z'^*ZZ-vertex in section IV C.

C. Goldstone boson Equivalence Theorem and R_ξ—independence

There are literally N-ways to derive the Ward Identities of Eq. (3). A classical method is to demand invariance of the path integral under the combined local vector and axial-vector gauge transformations (A9). We can then represent these WI's diagrammatically to prove the Goldstone Boson equivalence theorem [51–53]. This is most clearly explained in Lorentz gauge ($\xi = 0$) where the gauge fixing term (A10) does not involve the Goldstone boson field φ. Then conservation of the gauge current implies that q^μ can be contracted directly with $\Gamma^{\mu\nu\rho}$ and also with the derivatively coupled Goldstone boson to $\Gamma^{\nu\rho}$. In principle there is a third contribution from possible mixings with other gauge bosons, say Z', that couple to the same fermions in the vertex. This last mixing must necessarily be proportional to $(g_{\mu\lambda} - q_\mu q_\lambda/q^2)$ and when contracted with q^μ, vanishes. Therefore, by using rules from the toy model in Appendix A it is straightforward to see that we recover the classical WI (3a), without the anomalous term. While a possible gauge boson mixing contributes to $\Gamma^{\mu\nu\rho}$, it does not contribute to WIs in (3). At very high energy, the longitudinal polarization vector is $\varepsilon_{L\mu}(q) \simeq q_\mu/m_A$, where m_A is the gauge boson mass. In other words for an anomaly-free model, Eq. (3a) or the sum of the diagrams in Fig. 2, can be written as,

$$\epsilon_{L\mu}(q)\Gamma^{\mu\nu\rho} = i\Gamma^{\nu\rho}. \tag{11}$$

This equation tells us that at the high energy limit, the physical amplitude with the gauge boson in vertex μ is replaced by the vertex with a Goldstone boson that "has been eaten". However, as is evident from Eq. (3a), the relation (11) is broken by possible gauge anomalies. This is another reason why the latter should be absent.

One can easily check by studying, for example, the fermion-antifermion annihilation process to two gauge bosons with the toy model of Appendix A, that Eq. (11) is the required condition for the amplitude to be gauge ξ-independent. Again the anomalous term *must* be absent.

III. NONDECOUPLING EFFECTS

Heavy fermion nondecoupling effects can be cast in two classes:

(A) effects that arise from a large mass splitting between particles within an anomaly-free multiplet.

(B) *anomaly driven* effects that originate from decoupling a whole anomaly-free multiplet.

In case (A), formal decoupling of the heavy particle that participates in the anomaly cancellation mechanism will leave at low energies an effective Lagrangian $\Delta\Gamma^{\mu\nu\rho}$ that accounts for the anomaly cancellation missing piece [16,17,21]. In case (B) the Higgs coupling to fermions will be much larger than the gauge coupling with the latter being approximately zero when the fermion mass is going to infinity [28,29].

A. Non-decoupling due to large mass splitting

We are going to focus first on the simplest case with three external identical gauge bosons. This means we set $i = j = k$ in the Ward Identities of Eq. (3) or else we look directly at expressions, (B26)–(B28). In order to carry out a systematic study of nondecoupling effects and their interplay with chiral anomalies it is essential to keep track of the anomalous terms that depend on the arbitrary parameters w and z. By exploiting Bose symmetries for on-shell external gauge bosons, and specifically, (B39) among legs j and k we find $w = -z$, while with (B40) among legs i

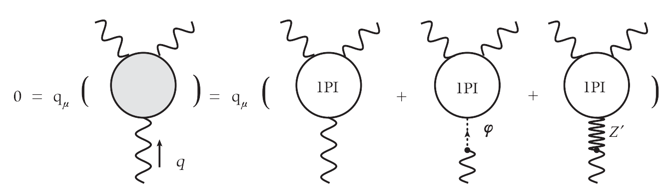

FIG. 2. Graphical representation of the WI in Eq. (3a).

and j we find (after some tedious algebra) $2w - z - 1 = 0$. The solution of this system,

$$w = -z = \frac{1}{3}, \tag{12}$$

finally fixes the arbitrary parameters w and z. Our observation is that these fixed values for the arbitrary parameters correspond to the case of a particle decoupling from the effective action, i.e.,

$$\lim_{m\to\infty} \Gamma^{\mu\nu\rho}(k_1, k_2; w, z) = 0 \Rightarrow w = -z = \frac{1}{3}. \tag{13}$$

We elaborate this point in what follows. The WIs now take the form:

$$q_\mu \Gamma^{\mu\nu\rho}(k_1, k_2; w = 1/3) = -\frac{e^3\beta m^2}{\pi^2}\varepsilon^{\lambda\nu\rho\sigma}k_{1\lambda}k_{2\sigma}I_0(k_1, k_2; m) + \frac{e^3(\beta^3 + 3\alpha^2\beta)}{6\pi^2}\varepsilon^{\lambda\nu\rho\sigma}k_{1\lambda}k_{2\sigma}. \tag{14a}$$

$$-k_{1\nu}\tilde{\Gamma}^{\nu\rho\mu}(k_1, k_2; w = 1/3) = -\frac{e^3\beta m^2}{\pi^2}\varepsilon^{\lambda\mu\rho\sigma}k_{1\lambda}k_{2\sigma}I_1(k_1, k_2; m) - \frac{e^3(\beta^3 + 3\alpha^2\beta)}{6\pi^2}\varepsilon^{\lambda\mu\rho\sigma}k_{1\lambda}k_{2\sigma}, \tag{14b}$$

$$-k_{2\rho}\hat{\Gamma}^{\rho\mu\nu}(k_1, k_2; w = 1/3) = -\frac{e^3\beta m^2}{\pi^2}\varepsilon^{\lambda\mu\nu\sigma}k_{1\lambda}k_{2\sigma}I_2(k_1, k_2; m) + \frac{e^3(\beta^3 + 3\alpha^2\beta)}{6\pi^2}\varepsilon^{\lambda\mu\nu\sigma}k_{1\lambda}k_{2\sigma}, \tag{14c}$$

where the integrals $I_{0,1,2}$ are defined in Eqs. (B5), (B22), and (B23) respectively. The anomalous terms in (14) are then allocated "democratically" in the three legs of $\Gamma^{\mu\nu\rho}$ as one would have naively expected. Note also that since $\lim_{m\to\infty} m^2 I_0 = -\lim_{m\to\infty} m^2 I_1 = \lim_{m\to\infty} m^2 I_2 = \frac{1}{6} \times (\beta^2 + 3\alpha^2)$ the r.h.s of Eqs. (14a)–(14c) cancels identically, verifying our statement in Eq. (13). Therefore, for a Dirac fermion pair circulating the loop as shown in Fig. 1 and for three identical external gauge bosons, *at the formal decoupling limit, the finite contributions are equal and opposite to the anomaly contributions in the vertex*. In a Lorentz gauge, terms in $\Gamma^{\mu\nu\rho}$ proportional to $I_{0,1,2}$ arise from the mixing between the Goldstone boson φ and the gauge boson as it is shown in Fig. 2. We should notice however, that our calculation of WIs in (14) given in Appendix B contains no reference to a particular gauge choice.

For a Lorentz-invariant and renormalizable chiral gauge theory the anomalous terms i.e., the last terms on the r.h.s of Eqs. (14), have to be absent. The only way,[3] consistent with renormalizability[4] [14,15], to remove the anomaly terms, is to add a new Dirac fermion pair with opposite β i.e., opposite hypercharges Y_L and Y_R. A consistent way to describe heavy fermion decoupling effects is to perform the calculation directly in the broken phase of the theory where physical masses appear explicitly. Assuming that the mass of the second (heavy) pair and the energy, $s = (k_1 + k_2)^2$, is much bigger than the first (light) fermion pair, say, $m_2^2 \gg s \gg m_1^2 \approx 0$, there is a nondecoupled term in the 1PI effective action which can be read off from Eqs. (B32), (B37), and (B38) [or Eqs. (2) and (4) for $i = j = k$] to be,

$$\Delta\Gamma^{\mu\nu\rho}(k_1, k_2) \approx \frac{e^3(\beta^3 + 3\alpha^2\beta)}{6\pi^2}\varepsilon^{\mu\nu\rho\sigma}(k_1 - k_2)_\sigma. \tag{15}$$

This term remains in the 1PI effective function for the light particle. In the heavy mass limit ($m_2 \to \infty$), the form factors $A_{i=3,\ldots 6}(k_1, k_2)$ vanish as $1/m^2$ leaving only the term (15) in the low energy effective action which has no "memory" anymore from the heavy mass m_2. Although, the exact nonkinematic prefactor in Eq. (15), depends upon model details, its magnitude (in e-units) is approximately, α/π and could be observable. Furthermore, the nondecoupling term (15) does not depend on the regularization scheme, i.e., on the parameters w and z in Eqs. (B37) and (B38), since the model is by construction anomaly-free.

B. Anomaly driven nondecoupling effects

This is a category of possible nondecoupling effects for models possessing an anomaly-free cluster of heavy particles just above those known from the SM. We systematically then check anomaly cancellation conditions in Ward Identities (3) by demanding the prefactors of $I_{1,2}$ integrals in Eqs. (4a) and (4b) to be nonzero. We are seeking for minimal models with up-to three different gauge bosons and up to the least n-Dirac fermions.

A model that contains one gauge boson X, with V-A couplings as in Eq. (1), coupled to only one fermion is impossible to exist because it is anomalous (except the trivial case of a vectorlike particle where $\beta = 0$). Adding an extra fermion with the same mass but with opposite axial-vector coupling (β) renders the model anomaly-free. Such a simple particle content does not lead to nondecoupling effects because all these effects are proportional to an odd power of the axial-vector coupling ($\sim \beta^{2k+1}$) and therefore the sum over the two fermions vanishes. Similar situation arises when more fermions are circulating in the loop.

More interesting is the case where one has two, distinct, external gauge bosons, X and Y, either massive or

[3] Of course there is the trivial case of vector multiplets i.e., $\beta = 0$.

[4] We are not going to consider here the situation [30] of incorporating nonrenormalizable counterterms to cancel the anomalies at the expense of introducing a cut-off scale $\Lambda \sim 4\pi v$.

massless. The cancellation of trilinear anomalies requires the existence of at least two fermions with opposite axial-vector couplings but again it is impossible to satisfy instantaneously the mixed anomaly and nondecoupling conditions [see below]. We first obtain the general conditions for an anomaly-free model with two gauge bosons X and Y. In notation of Eq. (1) these conditions read,

$$\sum_{i=1}^{n}(\beta_X^3 + 3\alpha_X^2\beta_X)_i = 0, \tag{16a}$$

$$\sum_{i=1}^{n}(\beta_Y^3 + 3\alpha_Y^2\beta_Y)_i = 0, \tag{16b}$$

$$\sum_{i=1}^{n}(\beta_X^2\beta_Y + 2\alpha_X\alpha_Y\beta_X + \alpha_X^2\beta_Y)_i = 0, \tag{16c}$$

$$\sum_{i=1}^{n}(\beta_Y^2\beta_X + 2\alpha_X\alpha_Y\beta_Y + \alpha_Y^2\beta_X)_i = 0, \tag{16d}$$

where n is the total number of fermions. Starting from trilinear anomalies (16a) or (16b) we see that the case $n = 1$ requires only vectorial couplings, $\beta_X = \beta_Y = 0$. Therefore for $n = 1$ there is no nontrivial solution. For $n = 2$ the nonzero couplings must satisfy the following conditions:

$$\beta_{X2} = -\beta_{X1}, \qquad \alpha_{X2} = \pm\alpha_{X1} \qquad \beta_{Y2} = -\beta_{Y1}, \qquad \alpha_{Y2} = \pm\alpha_{Y1}. \tag{17}$$

Turning to mixed anomalies (16c) and (16d), it is amusing first to note that they are satisfied even with one internal fermion ($n = 1$), iff

$$\beta_X = \alpha_X, \qquad \beta_Y = -\alpha_Y, \tag{18}$$

or

$$\beta_X = -\alpha_X, \qquad \beta_Y = \alpha_Y. \tag{19}$$

Nondecoupling conditions are derived by the requirement that the prefactors of I_1 and I_2 integrals in Eqs. (4a) and (4b) are nonzero. Hence, in the limit of $k_1^2, k_2^2 \simeq s \ll m^2$ at least one of the following algebraic expressions,

$$\sum_{i=1}^{n}(\beta_X^2\beta_Y + 3\alpha_X\alpha_Y\beta_X)_i, \qquad \sum_{i=1}^{n}(\beta_X^2\beta_Y + 3\alpha_X^2\beta_Y)_i,$$
$$\sum_{i=1}^{n}(\beta_Y^2\beta_X + 3\alpha_X\alpha_Y\beta_Y)_i, \qquad \sum_{i=1}^{n}(\beta_Y^2\beta_X + 3\alpha_Y^2\beta_X)_i, \tag{20}$$

must be nonvanishing. For $n = 1$ the choice (18) [or (Eq. (19))] which eliminates the mixed anomalies sets also Eqs. (20) to a nonzero value. However, to cancel the XXX and YYY anomalies one needs at least $n = 2$ fermions to satisfy the conditions (17). These set the nondecoupling expressions (20) back to zero. The first nontrivial solution of the system Eqs. (16) and (20) arises with three pairs of chiral Dirac fermions ($n = 3$) with an example of quantum numbers given in Table I. Here, we use (18) and (19) to cancel mixed anomalies for ψ_1. The other two particles ψ_2 and ψ_3 are singlets under $U(1)_Y$ and $U(1)_X$, respectively. Plug these into Eqs. (B32), (4), and (7), we obtain the nonvanishing operators at the decoupling limit:

TABLE I. Charges of an anomaly-free model with nondecoupling remnants in three gauge boson vertices XXY and YYX.

	ψ_1	ψ_2	ψ_3
$U(1)_X$	$\alpha = e,\ \beta = -e$	$\alpha = e,\ \beta = e$	$\alpha = 0,\ \beta = 0$
$U(1)_Y$	$\alpha = -e,\ \beta = -e$	$\alpha = 0,\ \beta = 0$	$\alpha = e,\ \beta = e$

$$\Gamma^{\mu\nu\rho}_{XYY} = \Gamma^{\mu\nu\rho}_{YXX} = \frac{e^3}{3\pi^2}\varepsilon^{\mu\nu\rho\sigma}(k_2 - k_1)_\sigma, \tag{21a}$$

$$\Gamma^{\mu\nu\rho}_{XYX} = \Gamma^{\mu\nu\rho}_{YXY} = -\frac{e^3}{3\pi^2}\varepsilon^{\mu\nu\rho\sigma}(2k_2 + k_1)_\sigma, \tag{21b}$$

$$\Gamma^{\mu\nu\rho}_{XXX} = \Gamma^{\mu\nu\rho}_{YYY} = 0. \tag{21c}$$

Next is a model example with $n = 4$ Dirac fermions charged under the product of gauge groups $U(1)_X \times U(1)_Y$. This toy model has been examined in Ref. [28]. Charge assignments are given in Table II. They are chosen in such a way that triangular anomalies $[U(1)_X]^3$ and $[U(1)_Y]^3$ are canceled separately. The cancellation of mixed anomalies requires the extra condition $q_2 = q_1\frac{(e_1^2 - e_2^2)}{(e_3^2 - e_4^2)}$. Charges in Table II follow the general rules of Eqs. (17). If we assume that all extra fermions have a common mass m and are all very heavy, then in the low energy limit we find the following expressions for the effective vertices with different combinations of external gauge bosons:

$$\Gamma^{\mu\nu\rho}_{XXX} = \Gamma^{\mu\nu\rho}_{YYY} = 0, \tag{22a}$$

$$\Gamma^{\mu\nu\rho}_{XXY} = \frac{q_1(e_1^2 - e_2^2)}{4\pi^2}(2k_1 + k_2)_\sigma\varepsilon^{\mu\nu\rho\sigma}, \tag{22b}$$

$$\Gamma^{\mu\nu\rho}_{YXX} = \frac{q_1(e_1^2 - e_2^2)}{4\pi^2}(k_2 - k_1)_\sigma\varepsilon^{\mu\nu\rho\sigma}, \tag{22c}$$

$$\Gamma^{\mu\nu\rho}_{XYY} = \Gamma^{\mu\nu\rho}_{YXY} = 0. \tag{22d}$$

These contributions arise from terms that are proportional to I_1 and I_2-integrals when taking into account that this model is anomaly-free. Such a situation should never occur in the SM. The basic difference is that neither gauge bosons X and Y is purely vectorlike for the entire fermionic sector i.e., X and Y must be *strictly massive*. This is a crucial difference that leads to the existence of remnants in the low energy limit. On the contrary, the existence of the photon in the SM leads to a term related to I_1 or I_2 which always vanishes for an anomaly-free model.

We have also worked out the case with three different gauge bosons. The corresponding 10 independent anomaly-free, and, 18 independent nondecoupling conditions, are quite involved and are presented separately in Appendix E. Again the nondecoupling effects arise for

TABLE II. Charges of all fermions with respect to the gauge groups $U(1)_X \times U(1)_Y$.

	ψ_1	ψ_2	χ_1	χ_2
$U(1)_X$	$\alpha = e_1,\ \beta = 0$	$\alpha = e_2,\ \beta = 0$	$\alpha = \frac{e_3+e_4}{2},\ \beta = \frac{e_3-e_4}{2}$	$\alpha = \frac{e_3+e_4}{2},\ \beta = -\frac{e_3-e_4}{2}$
$U(1)_Y$	$\alpha = 0,\ \beta = -q_1$	$\alpha = 0,\ \beta = q_1$	$\alpha = q_2,\ \beta = 0$	$\alpha = -q_2,\ \beta = 0$

$n \geq 3$. The new feature that appear in this category is the fact that one can exploit nondecoupling effects where one of the gauge bosons is massless. Such a minimal ($n = 3$) example comes into sight if we adopt the charge assignments shown in Table III. Notice that all fermions have $\beta_Y = 0$ i.e., the Y couples purely to a vector current. We can easily check that the conditions (E1) for an anomaly-free model are satisfied while at the same time some of the expressions in (E2) are nonzero. The nonzero effective vertices can be written in the form,

$$\Gamma^{\mu\nu\rho}_{XXZ} = -\Gamma^{\mu\nu\rho}_{ZZX} = \frac{e^3}{3\pi^2}(2k_1 + k_2)_\sigma \varepsilon^{\mu\nu\rho\sigma}, \tag{23a}$$

$$\Gamma^{\mu\nu\rho}_{XZX} = -\Gamma^{\mu\nu\rho}_{ZXZ} = -\frac{e^3}{3\pi^2}(2k_2 + k_1)_\sigma \varepsilon^{\mu\nu\rho\sigma}, \tag{23b}$$

$$\Gamma^{\mu\nu\rho}_{ZXX} = -\Gamma^{\mu\nu\rho}_{XZZ} = \frac{e^3}{3\pi^2}(k_1 - k_2)_\sigma \varepsilon^{\mu\nu\rho\sigma}, \tag{23c}$$

$$\Gamma^{\mu\nu\rho}_{YXZ} = \Gamma^{\mu\nu\rho}_{YZX} = \frac{e^3}{2\pi^2}(k_1 + k_2)_\sigma \varepsilon^{\mu\nu\rho\sigma}, \tag{23d}$$

$$\Gamma^{\mu\nu\rho}_{XYZ} = -\Gamma^{\mu\nu\rho}_{ZYX} = \frac{e^3}{2\pi^2} k_{1_\sigma} \varepsilon^{\mu\nu\rho\sigma}, \tag{23e}$$

$$\Gamma^{\mu\nu\rho}_{XZY} = \Gamma^{\mu\nu\rho}_{ZXY} = -\frac{e^3}{2\pi^2} k_{2_\sigma} \varepsilon^{\mu\nu\rho\sigma}. \tag{23f}$$

As an example, we observe that heavy fermion nondecoupling effects appear in Eqs. (23e) and (23f). If a model like this with $X = Z'$, $Y = \gamma$, $Z = Z$ can be embedded in the SM, then it would in principle allow for decays like $Z' \to Z\gamma$ that do not depend on the heavy fermion masses.

We should finally remark that in models considered in Tables I, II, and III, gravitational anomalies cancel out since it is always $\sum_f \beta^X_f = 0$ for a given axial vector coupling between a vector boson X and a fermion f.

IV. APPLICATIONS

A. Standard model

Focusing first in the SM with neutral, Z or γ triple gauge boson vertices we need only to consider the interaction Lagrangian with fermions. This reads as

TABLE III. Charges of an anomaly-free model with nondecoupling remnants in three gauge boson vertex XYZ.

	ψ_1	ψ_2	ψ_3
$U(1)_X$	$\alpha = e,\ \beta = e$	$\alpha = e,\ \beta = -e$	$\alpha = 0,\ \beta = 0$
$U(1)_Y$	$\alpha = e,\ \beta = 0$	$\alpha = e,\ \beta = 0$	$\alpha = e,\ \beta = 0$
$U(1)_Z$	$\alpha = e,\ \beta = -e$	$\alpha = 0,\ \beta = 0$	$\alpha = e,\ \beta = e$

$$\mathcal{L}_{\rm int} = \sum_f \alpha^\gamma_f A_\mu \bar{\Psi}_f \gamma^\mu \Psi_f + \sum_f Z_\mu \bar{\Psi}_f \gamma^\mu (\alpha^Z_f + \beta^Z_f \gamma_5)\Psi_f, \tag{24}$$

where the factors α^V_f, β^V_f with $V = \gamma, Z$ are

$$\alpha^\gamma_f = eQ_f, \qquad \beta^\gamma_f = 0,$$
$$\alpha^Z_f = \frac{g_Z}{2}(T^3_{f_L} - 2s^2_w Q_f), \qquad \beta^Z_f = -\frac{g_Z}{2}T^3_{f_L}, \tag{25}$$

and $T^3_{f_L}$ and Q_f are the third component of weak isospin and charge of the SM Dirac fermions $f = \nu, e, u, d$, respectively. Explicitly in the SM, the prefactors α^V_f and β^Z_f take the form:

$$\alpha^\gamma_u = \frac{2}{3}e, \qquad \alpha^Z_u = \frac{g_Z}{2}\left(\frac{1}{2} - \frac{4}{3}s^2_w\right), \qquad \beta^Z_u = -\frac{g_Z}{4},$$
$$\alpha^\gamma_d = -\frac{1}{3}e, \qquad \alpha^Z_d = \frac{g_Z}{2}\left(-\frac{1}{2} + \frac{2}{3}s^2_w\right), \qquad \beta^Z_d = \frac{g_Z}{4},$$
$$\alpha^\gamma_e = -e, \qquad \alpha^Z_e = \frac{g_Z}{2}\left(-\frac{1}{2} + 2s^2_w\right), \qquad \beta^Z_e = \frac{g_Z}{4}$$
$$\alpha^\gamma_\nu = 0, \qquad \alpha^Z_\nu = \frac{g_Z}{4}, \qquad \beta^Z_\nu = -\frac{g_Z}{4}, \tag{26}$$

where $g_Z = e/s_w$ is the weak boson gauge coupling and s_w, c_w are the sinus and cosinus of the weak mixing angle.

1. V^*ZZ

Our first application refers to the vertex V^*ZZ with $V = \gamma$, Z being off-shell. This interaction has been searched for at LEP and Tevatron while is currently under scrutiny at the LHC. At one-loop level the only CP-conserving contribution arises from the triangle graph in Fig. 1. Applying our general form of the 1PI vertex in Eq. (2) and making use of the Bose symmetry $\nu \leftrightarrow \mu$, $k_1 \leftrightarrow k_2$ as in Eq. (B39), we find

$$\Gamma^{\mu\nu\rho}_{V^*ZZ}(k_1, k_2; w) = \left[\epsilon^{\mu\nu\rho\sigma}(k_1 - k_2)_\sigma\left(-A_1 + \frac{s}{2}A_3\right) + A_3 q^\mu \epsilon^{\rho\beta\nu\delta} k_{1\beta} k_{2\delta}\right], \tag{27}$$

where the polarization vectors $\epsilon^*_\nu(k_1)\epsilon^*_\rho(k_2)$ outside the square brackets have been omitted, and also, we set $A_1 \equiv A_1(k_1, k_2)\ldots$ etc. for simplicity. More specifically, A_1 is ambiguous: it depends on how the momentum is routing the loop i.e., the parameter w. This arbitrariness (or regularization scheme dependence if you wish) is further fixed by exploiting the fact that the ZZZ on-shell boson vertex vanishes by Bose symmetry. The latter requires $w = 1/3$. On the other hand for the vertex γZZ, conservation of the vector current and Bose symmetry implies that $w = z = 0$.

Having specified the arbitrary parameters w and z we apply our general expressions for A_1 and A_3 found in Eqs. (4a) and (8a), specifically to the vertices Z^*ZZ and γ^*ZZ and sum over all SM fermions. By ignoring (see below however), the last term proportional to q^μ in Eq. (27), we can easily find,

$$\Gamma^{\mu\nu\rho}_{Z^*ZZ}(k_1, k_2) = \epsilon^{\mu\nu\rho\sigma}(k_1 - k_2)_\sigma \sum_{f=u,d,e,\nu}\Big[m_Z^2(A_{3f} - A_{4f}) + \frac{m_f^2\beta_f^Z}{\pi^2}I_{1f} + \frac{1}{6\pi^2}(\beta_f^{Z3} + 3\beta_f^Z\alpha_f^{Z2})\Big] \equiv \epsilon^{\mu\nu\rho\sigma}(k_1 - k_2)_\sigma\Gamma_{Z^*ZZ}(s), \tag{28}$$

$$\Gamma^{\mu\nu\rho}_{\gamma^*ZZ}(k_1, k_2) = \epsilon^{\mu\nu\rho\sigma}(k_1 - k_2)_\sigma \sum_{f=u,d,e,\nu}\Big[m_Z^2(A_{3f} - A_{4f}) + \frac{m_f^2\beta_f^Z}{\pi^2}I_{1f} + \frac{1}{2\pi^2}\alpha_f^\gamma\alpha_f^Z\beta_f^Z\Big] \equiv \epsilon^{\mu\nu\rho\sigma}(k_1 - k_2)_\sigma\Gamma_{\gamma^*ZZ}(s), \tag{29}$$

where $s = (k_1 + k_2)^2$ and I_{1f} is given by Eq. (5a). The last term in Eqs. (28) and (29) is the anomaly contribution, while the second term is a nondecoupling one in the limit of heavy fermion mass, $m_f \to \infty$. Again we should notice here that in this limit and for one fermion contribution, the last two terms mutually cancel while the first term vanishes as m_Z^2/m_f^2. Therefore, the decoupling of heavy fermions in V^*ZZ vertex is operative even if those fermions have vastly different, but always much greater than the EW scale, masses among each other. In the SM,, for example, what is left behind after the decoupling of the top quark is a theory with an anomalous (sometimes called *Chern-Simons*) term that is necessary to render the effective low energy theory gauge invariant.

Especially for γ^*ZZ one can go one step further and write the whole effective vertex in terms of one integral only, namely

$$\Gamma_{\gamma^*ZZ}(s) = \frac{s}{2}\sum_{f=u,d,e,\nu} A_{3f}(s). \tag{30}$$

Now bringing back the last term on the r.h.s of Eq. (27) we find a perfectly fine and gauge invariant form for γ^*ZZ-vertex

$$\Gamma^{\mu\nu\rho}_{\gamma^*ZZ}(s) = \sum_f \frac{sA_{3f}}{2}\Big[\epsilon^{\mu\nu\rho\sigma}(k_1 - k_2)_\sigma - \frac{\epsilon^{\nu\rho\beta\sigma}q^\mu q_\beta}{s}(k_1 - k_2)_\sigma\Big]. \tag{31}$$

This vertex *must* be proportional to s in order to cancel the pole contribution arising at $s = q^2 = 0$ [36]. This is a generic statement for all γ^*VV vertices we address below. One should recall that this expression has been derived only after fixing the anomaly coefficients, w and z, by symmetry requirements. We could have done the reverse: to fix w, z from the requirement of no pole contribution in Eq. (31). In a way, the anomaly and the nondecoupled terms have been absorbed in the finite integral A_3. It is now evident from Eqs. (30) and (8) that $\Gamma_{\gamma^*ZZ}(s \to 0) = 0$ for every fermion contribution, independently. Furthermore, as expected, for asymptotic values of s we also observe, $\Gamma_{\gamma^*ZZ}(s \to \infty) = 0$, after summing over all SM fermion contributions.

Within one generation of fermions, the SM is a chiral, gauge, and, anomaly-free Quantum Field Theory (QFT). As a result, contributions to Γ_{V^*ZZ} from (approximately) massless generations, vanish identically (recall that form factors $A_{3,4}$ are proportional to the anomaly factors, [see Eqs. (8a) and (8b)] and the second term vanishes in the massless case). Therefore to a good approximation, for $\sqrt{s} \gtrsim 2M_Z$, the only non-negligible contribution to Γ_{V^*ZZ} arises from the third generation and is due to the large mass difference between the top quark and all other fermions. The top quark influences mainly the last two terms in the square bracket of Γ_{Z^*ZZ} and Γ_{γ^*ZZ} in Eqs. (28) and (29). If we make the (numerically crude) approximation of $m_Z^2 \ll s < m_t^2$ and exploit Eq. (D12c) from the Appendix D we find ($N_c = 3$ is the color factor),

$$\frac{m_t^2\beta_t^Z}{\pi^2}I_{1t} \approx -\frac{N_c}{6\pi^2}(\beta_t^{Z3} + 3\beta_t^Z\alpha_t^{Z2}) - \frac{N_c}{120\pi^2}(\beta_t^{Z3} + 5\beta_t^Z\alpha_t^{Z2})\frac{s}{m_t^2}. \tag{32}$$

The first term is just the opposite of the top quark anomaly contribution in Γ_{Z^*ZZ} and they both cancel out in the limit of heavy top quark. One can prove easily this statement for all SM vertices, Γ_{V^*VV}, $V = Z, \gamma$ appearing below in this article and we claim, following the arguments of Sec. III, that this is a general theorem: *a heavy particle cancels its own anomaly contribution in a triple gauge boson vertex and at the (nonperturbative) limit of $m \to \infty$ leaving no trace from itself behind*. Of course in the topless SM the last term in Γ_{Z^*ZZ} does not vanish since the particle content (τ, ν_τ, b) is now anomalous. It is also evident from Eq. (32) that the behavior of $\Gamma_{Z^*ZZ}(s)$ at $s \approx m_t^2$ rises approximately linearly with s as s/m_t^2. This is also verified from our numerical results shown in Fig. 3(a). Similar conclusions one can derive for Γ_{γ^*ZZ} and Fig. 3(b) but this is rather obvious now because of Eq. (30).

Furthermore, it is also instructive to study the behavior of the vertices $\Gamma_{V^*ZZ}(s)$ in the asymptotic region, $s \gg m_t^2 > m_Z^2$. By exploiting Eq. (D13) and keeping only terms of order m_f^2/s we arrive at the following expression,

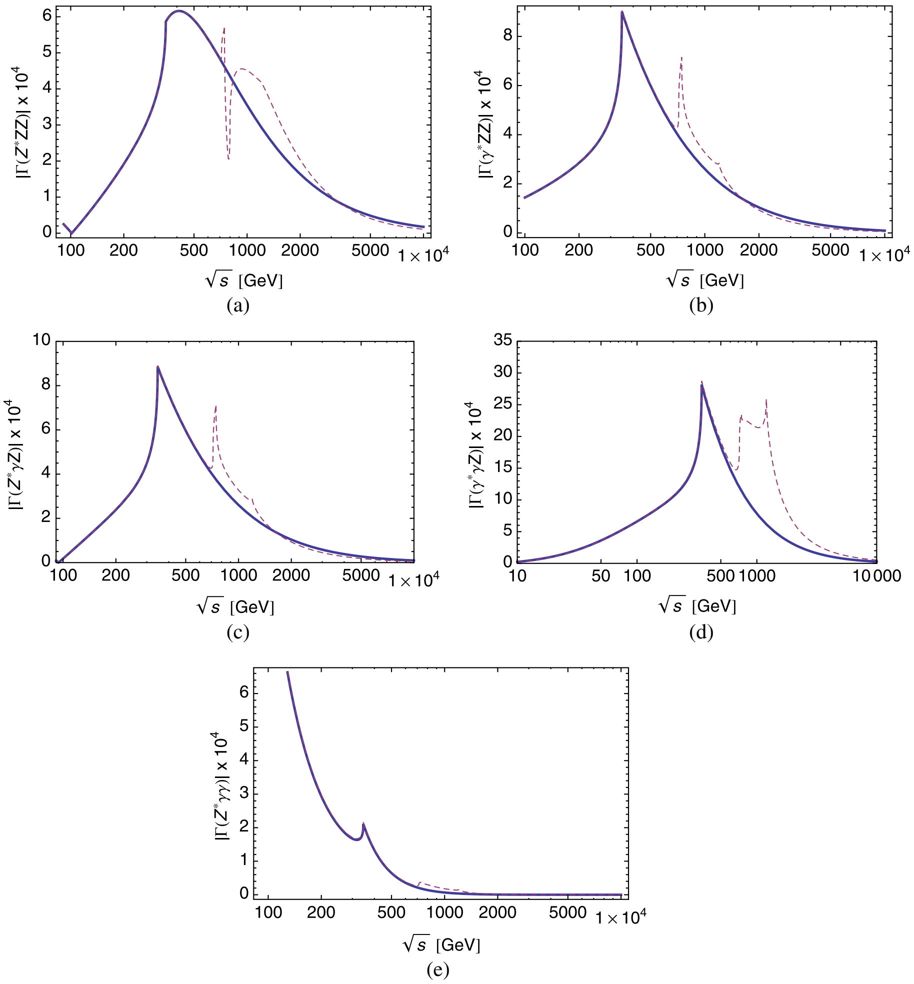

FIG. 3 (color online). The dependence of $|\Gamma_{V^*VV}(s)|$ with $\sqrt{s}$ for different gauge bosons combinations, $V = \gamma, Z$: (a) Z^*ZZ, (b) γ^*ZZ, (c) $Z^*\gamma Z$, (d) $\gamma^*\gamma Z$, (e) $Z^*\gamma\gamma$. The solid curve corresponds to the SM, the dashed curve corresponds to the SM + 4th fermion generation model. Masses for light quarks and leptons are neglected while $m_t = 173$ GeV. Fourth generation quarks and lepton masses are taken as in (66).

$$\Gamma_{Z^*ZZ}(s \gg m_t^2) \approx N_c \frac{m_t^2}{s}\left\{\frac{2\beta_t^{Z3}}{\pi^2}\left(2 - \ln\frac{s}{m_t^2} - i\pi\right) + \frac{\beta_t^{Z3} + \alpha_t^{Z2}\beta_t^Z}{\pi^2}\left(\frac{1}{2}\ln^2\frac{s}{m_t^2} - \frac{\pi^2}{2} + i\pi\ln\frac{s}{m_t^2}\right)\right\}, \tag{33}$$

in which both real and imaginary parts vanish at asymptotic values of s as they should following unitarity arguments. The effect of a "heavy" particle (here the top quark) is to just delay the "falling off" of $|\Gamma_{Z^*ZZ}(s)|$ [see Fig. 3(a).] as $s \to \infty$. Finally, it is also obvious that the real and imaginary part of Γ_{Z^*ZZ} are of the same order of magnitude, a situation which remains true everywhere after the threshold energy, $s \gtrsim 4m_t^2$.

Translating our numerical results for the SM to the notation of Ref. [36][5] that is usually followed by the theoretical and experimental literature, we find for $m_t = 173$ GeV and LEP energies, that

$$f_5^Z(\sqrt{s} = 200 \text{ GeV}) = 1.8 \times 10^{-4}, \tag{34}$$

$$f_5^\gamma(\sqrt{s} = 200 \text{ GeV}) = 2.1 \times 10^{-4}, \tag{35}$$

where we have neglected small imaginary part contributions from light quark and lepton mass thresholds. These results agree with those quoted in Ref. [42]. Unfortunately, they are too small to have been reached by LEP [54].

Just above the top quark threshold energies $s \gtrsim 4m_t^2$, the vertex develops a significant absorptive part. This is apparent from our analytical expressions in Appendix D for

[5]We multiply $\Gamma_{V^*ZZ}(s)$ in Eqs. (28) and (29) with $em_Z^2/(s - m_V^2)$.

integrals $A_{3\ldots6}$ and $I_{1,2}$ and the discussion above. For $\sqrt{s} = 500$ GeV we find:

$$f_5^Z(\sqrt{s} = 500\ \text{GeV}) = (0.4 - 0.5i) \times 10^{-4}, \tag{36}$$

$$f_5^\gamma(\sqrt{s} = 500\ \text{GeV}) = (-0.3 + 0.3i) \times 10^{-4}. \tag{37}$$

Note again that the imaginary part of the amplitude is of the same order of magnitude as the real part.

2. $V^*\gamma Z$

Another nontrivial class among trilinear neutral gauge boson vertices that have been and being searched for at colliders is the amplitude $V^*\gamma Z$. In the notation of Fig. 1, we assign $V^*_\mu(q)$, $\gamma_\nu(k_1)$ and $Z_\rho(k_2)$ to the 1PI effective vertex $\Gamma^{\mu\nu\rho}_{V^*\gamma Z}$ of Eq. (2) with $V = Z, \gamma$. When the photon and the Z-gauge boson are both on-shell we find:

$$\begin{aligned}\Gamma^{\mu\nu\rho}_{V^*\gamma Z}(k_1, k_2) = {}& \epsilon^{\mu\nu\rho\sigma} k_{1\sigma}\left(A_2 + \frac{s + m_Z^2}{2} A_3\right) \\ &+ \epsilon^{\mu\rho\beta\delta} q^\nu q_\beta k_{2\delta}(A_3 + A_6) \\ &+ \epsilon^{\nu\rho\beta\delta} q^\mu k_{1\beta} k_{2\delta} A_3.\end{aligned} \tag{38}$$

We have seen however in Eq. (8d) that $A_3 = -A_6$ and therefore, the second term in Eq. (38) vanishes at one-loop. Furthermore, the last term when coupled to a light quark or lepton vector current, is proportional to the mass of the incoming fermions and for current collider architectures this contribution is negligible.[6] Hence, only the first term remains with potentially visible effects. When *all* external particles are on-shell, Bose symmetry and gauge invariance require the vertex $V\gamma Z$ to vanish. Bose symmetry relations among form factors and gauge invariance fix the arbitrary parameters w and z to be:

$$Z\gamma Z\colon\ w = 1, \qquad z = 0, \tag{39}$$

$$\gamma\gamma Z\colon\ w = 1, \qquad z = 1. \tag{40}$$

By substituting the form in A_2 from the general expression of (4b) we obtain:

$$\begin{aligned}\Gamma^{\mu\nu\rho}_{Z^*\gamma Z}(k_1, k_2) = {}& \epsilon^{\mu\nu\rho\sigma} k_{1\sigma} \sum_{f=u,d,e,\nu}\left[m_Z^2(A_{3f} + A_{5f}) \right. \\ &\left. - \frac{m_f^2 \beta_f^Z}{\pi^2} I_{2f} + \frac{1}{2\pi^2}\alpha_f^Z \alpha_f^\gamma \beta_f^Z \right] \\ \equiv {}& \epsilon^{\mu\nu\rho\sigma} k_{1\sigma} \Gamma_{Z^*\gamma Z}(s),\end{aligned} \tag{41}$$

[6] This term however is important for gauge invariance to be preserved, as in Eq. (31) before.

$$\begin{aligned}\Gamma^{\mu\nu\rho}_{\gamma^*\gamma Z}(k_1, k_2) = {}& \epsilon^{\mu\nu\rho\sigma} k_{1\sigma} \sum_{f=u,d,e,\nu}\left[m_Z^2(A_{3f} + A_{5f}) \right. \\ &\left. - \frac{m_f^2 \beta_f^Z}{\pi^2} I_{2f} + \frac{1}{2\pi^2}\alpha_f^\gamma \alpha_f^\gamma \beta_f^Z \right] \\ \equiv {}& \epsilon^{\mu\nu\rho\sigma} k_{1\sigma} \Gamma_{\gamma^*\gamma Z}(s).\end{aligned} \tag{42}$$

One should notice that the square bracket of $\Gamma_{Z^*\gamma Z}$ is approximately equal to $\Gamma_{\gamma^* ZZ}$ since in this case $A_5 \simeq -A_4$ and $I_1 \simeq -I_2$.

It is amusing to see how greatly the $\gamma^*\gamma Z$-vertex is simplified. Placing back the last term of Eq. (38) in order to restore gauge invariance, we find,

$$\Gamma^{\mu\nu\rho}_{\gamma^*\gamma Z}(s) = \sum_f s A_{3f} \times \left[\epsilon^{\mu\nu\rho\sigma} k_{1\sigma} - \frac{\epsilon^{\nu\rho\beta\sigma} q^\mu k_{2\beta} k_{1\sigma}}{s} \right]. \tag{43}$$

The s-factor outside the vertex is expected because it must cancel the pole behavior of the second term in the square bracket. Once again, the "physical" choice of w, z in the anomalous terms played a crucial role in Eq. (43) like in the case of $\gamma^* ZZ$ vertex. Regarding decoupling effects, Eq. (43) is self explained: for every particle contribution, a synergy between anomalous and nondecoupling terms results in a well defined integral sA_{3f} that vanishes asymptotically due to the anomaly-free condition. If however, the energy $\sqrt{s}$ is between two particle masses which combined render the model anomaly-free then there should be nondecoupling effects in this regime. One the other hand, adding to the SM, anomaly-free and heavy chiral fermions, there should be no-nondecoupling effects remaining in the low energy regime where $\sqrt{s} \lesssim 2m_t$.

One can go one step further also in the case of $Z^*\gamma Z$ of Eq. (41). In fact, we can eliminate I_{2f} and the anomaly factors from Eq. (41) leaving only the finite integrals A_3 and A_5, as

$$\Gamma_{Z^*\gamma Z}(s) = \frac{1}{2}\sum_f [(s + m_Z^2) A_{3f} + m_Z^2 A_{5f}]. \tag{44}$$

After using few integral tricks, like, for example, the ones of Eq. (B44), it is easy to show that $\Gamma_{Z^*\gamma Z}(s)$ behaves like $(s - m_Z^2)A_{3f}$ near the Z-pole. In general, $\Gamma_{V^*\gamma Z} \propto \sum_f (s - m_V^2) A_{3f}$ near the pole, is clearly verified when performing the full numerical evaluation of the integrals as in Figs. 3(c) and 3(d).

One can easily see from further working out Eqs. (41) and (42) that due to the fact that the SM is an anomaly-free QFT, the whole contribution arises to a very good approximation from particles of the third generation. Numerically, in the conventions of Ref. [36] [see also footnote 4], we find for LEP energies

$$h_3^Z(\sqrt{s} = 200\ \text{GeV}) = 2.1 \times 10^{-4}, \tag{45}$$

$$h_3^\gamma(\sqrt{s} = 200\ \mathrm{GeV}) = 7.2 \times 10^{-4}, \tag{46}$$

up to tiny small imaginary parts. These results are in agreement with those presented in Ref. [42]. As we have noticed above, it is also confirmed numerically that $|f_5^\gamma| \simeq |h_3^\gamma|$. SM predictions of Eqs. (47) and (48) are in the best case [for h_3^γ] 2 orders of magnitude below the published LEP bounds [54].

For comparison, at higher energies the SM predicts:

$$h_3^Z(\sqrt{s} = 500\ \mathrm{GeV}) = (0.3 - 0.6i) \times 10^{-4}, \tag{47}$$

$$h_3^\gamma(\sqrt{s} = 500\ \mathrm{GeV}) = (0.9 - 1.8i) \times 10^{-4}. \tag{48}$$

Full numerical results for $|\Gamma_{V^*\gamma Z}(s)|$ are represented by solid lines in Figs. 3(c) and 3(d). We observe that in the neighborhood of the top threshold, $|\Gamma_{\gamma^*\gamma Z}(s)|$ is 1 order of magnitude bigger than $|\Gamma_{Z^*\gamma Z}(s)|$, but still in the region 10^{-3}. They are both however far below the current Tevatron and LHC sensitivity [55,56]. For example, both ATLAS [57] and CMS [58] experiments at LHC currently report bounds on trilinear, $V^*\gamma Z$, gauge boson vertices $|h_3^{Z,\gamma}|$ that in the best case are not less than 5%. These experiments present bounds w.r.t the scale Λ in which the new physics enters. Following the projecting sensitivity calculated in Ref. [40], and setting $\Lambda \sim m_t$ for the SM, LHC sensitivity for $V^*Z\gamma$ with $\sqrt{s} = 14$ TeV will not be better than $\sim 10^{-2}$ and this makes its observation extremely difficult within SM, even for $\gamma\gamma Z$-vertex.

3. $V^*\gamma\gamma$

We now turn our discussion to the last SM neutral triple gauge boson vertex, the $V^*\gamma\gamma$. Of course, thanks to Furry's theorem only the case $V = Z$ is valid (for $V = \gamma$ all three currents are vectorlike, i.e., $\beta_i = 0$). However, even in $Z^*\gamma\gamma$ there are no nondecoupling effects since there is no would be Goldstone boson associated with the unbroken $U(1)_{\mathrm{em}}$, i.e., the final particles are massless. Nevertheless one can write a simple $Z^*\gamma\gamma$ 1PI vertex. We obtain:

$$\Gamma^{\mu\nu\rho}_{Z^*\gamma\gamma}(k_1, k_2) = \epsilon^{\nu\rho\beta\delta} q^\mu k_{1\beta} k_{2\delta}[A_3] + \frac{\beta_f^Z (\alpha_f^\gamma)^2}{4\pi^2} \times \epsilon^{\mu\nu\rho\sigma}[(w-1)k_2 + (z+1)k_1]_\sigma. \tag{49}$$

Landau [59] and Yang [60] say that the on-shell amblitute, $\epsilon_\mu(q)\Gamma^{\mu\nu\rho}_{Z^*\gamma\gamma}(k_1, k_2)$ must vanish due to selection rules on space inversion and angular momentum conservation. This fixes the arbitrary parameters $w = -z = 1$ for every fermion contribution f. One obtains the same values for w and z from $U(1)_{\mathrm{em}}$ gauge invariance, i.e., satisfaction of Ward Identities. Although it is necessary to preserve gauge invariance, this remaining contribution is negligible for light s-channel incoming particles e.g., $e^+e^- \to \gamma\gamma$, but nevertheless it may be important for heavy external particles like, for example, dark matter particles or heavy neutrinos annihilating into photons (see related work in Refs. [61,62]).

Defining $\Gamma_{Z^*\gamma\gamma}(s) \equiv \sum_f m_Z^2 A_{3f}(s)$ and summing over the SM particles, we find numerically,

$$\Gamma_{Z^*\gamma\gamma}(\sqrt{s} = 200\ \mathrm{GeV}) = 2.9 \times 10^{-4}, \tag{50}$$

$$\Gamma_{Z^*\gamma\gamma}(\sqrt{s} = 500\ \mathrm{GeV}) = (3.2 - 5.6i) \times 10^{-5}. \tag{51}$$

For various values of s, the function $|\Gamma_{Z^*\gamma\gamma}(s)|$ is plotted in Fig. 3(e). Notably, at very small s this quantity behaves like $1/s$ and in contrary to the previous Z^*VV vertices does not vanish at $s = m_Z^2$. For general values of s, and $k_1^2 = k_2^2 = 0$, $\Gamma_{Z^*\gamma\gamma}(s)$ is easily written as

$$\Gamma_{Z^*\gamma\gamma}(s) = \sum_f \frac{\beta_f^Z (\alpha_f^\gamma)^2}{2\pi^2} \frac{m_Z^2}{s} \xi_f J(\xi_f), \tag{52}$$

where $\xi_f \equiv 4m_f^2/m_Z^2$ and the function $J(\xi_f)$ is appended in Eq. (D2). For energies (s) below the top quark threshold, $\Gamma_{Z^*\gamma\gamma}(s)$, approximately takes the form,

$$\Gamma_{Z^*\gamma\gamma}(s) \equiv \sum_f m_Z^2 A_{3f}(m_Z^2 < s < m_t^2) \approx -N_c \frac{\beta_t^Z \alpha_t^{\gamma 2}}{\pi^2}\left[\frac{m_Z^2}{2s} + \left(\frac{m_Z^2}{m_t^2}\right)\left(\frac{1}{24} + \frac{1}{180}\frac{s}{m_t^2}\right)\right], \tag{53}$$

a behavior which shows decoupling of a heavy top-quark mass. This follows our general statement just below Eq. (32): since the anomalous term in Eq. (49) vanishes due to the physical choice of w and z, there is no nondecoupled remnant to cancel it. In the asymptotic region we find

$$\Gamma_{Z^*\gamma\gamma}(s \gg m_Z^2, m_t^2) \approx N_c \frac{\beta_t^Z \alpha_t^{\gamma 2}}{2\pi^2}\left(\frac{m_Z^2 m_t^2}{s^2}\right) \times \left[\ln^2\frac{s}{m_t^2} - \pi^2 + 2i\pi \ln\frac{s}{m_t^2}\right]. \tag{54}$$

Therefore, $\Gamma_{Z^*\gamma\gamma}(s)$ behaves asymptotically as $1/s^2$, while all other neutral vertices behave like $1/s$. This fast drop with s is also verified by comparing the solid lines between Figs. 3(a)–3(e).

4. $V^*W^-W^+$

Just for completeness, we study the chiral CP-invariant part of the $(\gamma, Z)^*WW$ vertex. For on-shell W's and in momentum space this corresponds to operators of the form,

$$f_5^V \epsilon^{\mu\nu\rho\sigma}(k_1 - k_2)_\sigma. \tag{55}$$

There are of course CP-invariant, nonchiral operators generated from our fermion triangle graph that have the form [36,37],

$$f_1^V(k_1-k_2)^\mu g^{\nu\rho} - \frac{f_2^V}{m_W^2}(k_1-k_2)^\mu q^\nu q^\rho + f_3^V(q^\nu g^{\mu\rho} - q^\rho g^{\mu\nu}). \quad (56)$$

In the SM, note that both f_1 and f_3, exist at tree level. We are interested here only on chiral, one-loop (triangle) induced operators (55).

The numerical calculation of the $(\gamma^*, Z^*)W^-W^+$ effective vertices are somehow more complicated than the neutral ones. There are two masses and two different neutral vertices involved, making the triangle diagram looking differently than its crossed counterpart (see Fig. 4). We follow the same steps as we did for the neutral vertices and present our results (and technical details) in Appendix C. The chiral CP-invariant part of the effective vertex, $\Gamma^{\mu\nu\rho}$, is the same as in Eq. (2). The finite form factors $A_{3\ldots6}$ need to be slightly modified by the mass difference of the two fermions involved; analogously for $A_{1,2}$. Our main conclusion for a general vertex that contains external charged gauge bosons is given by Eqs. (C2) and (C3).

The relevant couplings $\alpha^W_{ff'}$, and $\beta^W_{ff'}$ can be read from the charged current part of the SM Lagrangian,

$$\mathcal{L} \supset g_Z(W^+_\mu J^{\mu+}_W + W^-_\mu J^{\mu-}_W), \quad (57)$$

with the $J^{\pm}_W$-currents being

$$J^{\mu+}_W = (J^{\mu-}_W)^\dagger = \frac{1}{2\sqrt{2}}[\bar{\nu}\gamma^\mu(1-\gamma_5)e + \bar{u}\gamma^\mu(1-\gamma_5)d]. \quad (58)$$

Hence $\alpha^W_{ff'} = -\beta^W_{ff'} = \frac{g_Z}{2\sqrt{2}}$ for the pairs $(ff') = (\nu, e)$, (u, d), respectively. For simplicity, we ignore quark and lepton mixing effects, but these can easily be included.

We therefore set $\alpha_{j,k} = -\beta_{j,k} = \frac{g_Z}{2\sqrt{2}}$ in Eqs. (C2) and (C3). The neutral gauge boson-fermion couplings, α^V_f, β^V_f, are taken from Eq. (26). Assuming CP-conservation, the 1PI effective action $\Gamma^{\mu\nu\rho}_{V^*WW}$ with $V = \gamma, Z$ looks exactly the same as in Eq. (27) with the only difference being the form factors $A_{1,3}$ must be replaced by those given in Eq. (C2) [and the paragraph below (C2)]. Therefore we write,[7]

$$\Gamma^{\mu\nu\rho}_{V^*W^-W^+}(k_1+k_2) \equiv \epsilon^{\mu\nu\rho\sigma}(k_1-k_2)_\sigma \Gamma_{V^*W^-W^+}(s), \quad (59)$$

where

$$\Gamma_{V^*W^-W^+}(s) = \sum_{\text{doublets}}\Big[m_W^2(A_3-A_4) + \frac{g_Z^2\alpha^V_{f_d}}{16\pi^2}\mathcal{I}_1 + \frac{g_Z^2\beta^V_{f_d}}{16\pi^2}\mathcal{I}_2 + \frac{g_Z^2}{32\pi^2}(\alpha^V_{f_d} - \beta^V_{f_d})(w-1) + (f_u \leftrightarrow f_d)\Big]. \quad (60)$$

In this formula we abbreviate $A_{3,4} \equiv A_{3,4}(m^2_{f_u}, m^2_{f_d})$ and $\mathcal{I}_{1,2} \equiv \mathcal{I}_{1,2}(m^2_{f_u}, m^2_{f_d})$, with

$$\mathcal{I}_1 = \int_0^1 dx \int_0^{1-x} dy \frac{-(x+y)\Delta m^2 + m^2_{f_u}}{x(x-1)m_W^2 + y(y-1)m_W^2 - xy(s-2m_W^2) - (x+y)\Delta m^2 + m^2_{f_u}} \quad (61a)$$

$$\mathcal{I}_2 = \int_0^1 dx \int_0^{1-x} dy \frac{2xm^2_{f_d} + (x+y)\Delta m^2 - m^2_{f_u}}{x(x-1)m_W^2 + y(y-1)m_W^2 - xy(s-2m_W^2) - (x+y)\Delta m^2 + m^2_{f_u}} \quad (61b)$$

where $\Delta m^2 \equiv m^2_{f_u} - m^2_{f_d}$. In the limit of heavy masses, $m^2 = m^2_{f_u} = m^2_{f_d} \gg s, m_W^2$, we obtain,

$$\lim_{m^2\to\infty}\mathcal{I}_1 = \frac{1}{2}, \qquad \lim_{m^2\to\infty}\mathcal{I}_2 = -\frac{1}{6}. \quad (62)$$

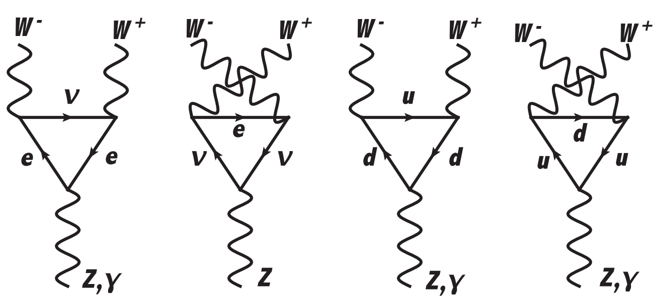

FIG. 4. SM fermion contributions to $(Z, \gamma)WW$ one-loop vertex.

Lets examine the $\gamma^*W^-W^+$ case first. We must set $\beta^\gamma_{f_{u,d}} = 0$. In this case gauge invariance [see Eq. (C4)] implies $w = z$ and CP-invariance $w = -z$, and therefore $w = z = 0$. Having fixed the anomalous term the result for this vertex turns out to be simply,

$$\Gamma_{\gamma^*W^-W^+}(s) = \frac{1}{2}s\sum_{\text{doublets}}[A_3(m^2_{f_u}, m^2_{f_d}) + (f_u \leftrightarrow fd)], \quad (63)$$

where A_3 is a form factor defined in the Appendix C. We should note here that $\Gamma_{\gamma^*W^-W^+}(s=0) = 0$ as it should be [36,37], i.e., there is no pole at $q^2 = 0$. This is a special

[7]Our notation for $\Gamma_{V^*W^-W^+}(s)$ is related to the standard form factor of Ref. [36], as $\Gamma_{V^*W^-W^+}(s) = -gVWWf^V_5(s)$.

case where the anomaly term conspires with I_1-term such that the final result contains no nondecoupling terms. In order for gauge invariance to be nonanomalous, the last terms in the WIs system (C4), must vanish. This implies a relation among fermion charges,

$$\sum_{f=e,\nu,d,u} \alpha_f^\gamma = Q_e + Q_\nu + 3Q_d + 3Q_u = 0, \qquad (64)$$

which is exactly the charge conservation condition. Then, in the asymptotic limit, $s \gg m_W^2, m_{f_{u,d}}^2$, the amplitude for $\Gamma_{\gamma^* W^- W^+}(s \to \infty)$ vanishes, thanks to Eq. (64). This is obvious from the numerical outcome in Fig. 5. It also shows an enhanced threshold behavior around $\sqrt{s} \approx 2m_t$ (solid line). Quantitatively, this can be seen from Eq. (63) by expanding A_3 around the threshold. Compared to $\Gamma_{\gamma^* ZZ}(s)$, there is an additional contribution due to the large mass difference $\Delta m^2 = m_t^2 - m_b^2 \approx m_t^2$, in the numerical factor that multiplies s/m_t^2. Our evaluation of integrals contains one numerical integration and follows the procedure of Appendix B in Ref. [5]. Our analytic formulae in Appendix D, at the limit of $m_W = 0$, are in full agreement with these results. Few representative values are,

$$\Gamma_{\gamma^* WW}(\sqrt{s} = 200\ \text{GeV}) = (6.8 - 6.4i) \times 10^{-4},$$
$$\Gamma_{\gamma^* WW}(\sqrt{s} = 500\ \text{GeV}) = (-1.5 + 15i) \times 10^{-4}.$$

Comparing with $\gamma^* ZZ$ vertex we see here that the mass splitting generates a sizeable absorptive part that dominates the vertex after $\sqrt{s} \gtrsim 2m_W$.

We now turn to the $Z^* W^- W^+$ vertex. This time we have only CP-symmetry at our disposal which sets only the constraint $w = -z$. At the broken limit there is no other symmetry remaining in order to fix the parameter w alone. However, in the exact $SU(2)$-limit, where $[q', s_w \to 0, \alpha_f = -\beta_f]$, this vertex should be exactly the same as the $Z^* ZZ$-vertex. There, the arbitrary parameters are fixed by Bose symmetry to be $w = -z = 1/3$. For this choice of w and at the heavy mass limit, $m^2 = m_{f_u}^2 = m_{f_d}^2 \gg s, m_W^2$, the vertex is proportional to $\alpha_f + \beta_f \propto s_w^2$, for every fermion contribution, which in turn is proportional to $SU(2)$-breaking effects. Another, equally good, choice would be $w = 0$, for example. The physical requirement here is the decoupling of a particle from the $\Gamma_{Z^* WW}$-vertex.

In conclusion, the $Z^* WW$ vertex is *undetermined*: there is only CP-symmetry, that is not enough to fix two arbitrary parameters. However, for the anomaly-free SM this arbitrariness is irrelevant since it is cancelled when the whole fermion contribution is taken into account. We shall meet this situation again in the $Z' VV$-vertex below.

Our numerical evaluation of the SM $|\Gamma_{Z^* WW}(s)|$ is shown in Fig. 6. This time, the top quark threshold destructively adds to the vertex. As in previous cases, we present few representative values,

$$\Gamma_{Z^* WW}(\sqrt{s} = 200\ \text{GeV}) = -(8.5 + 7.6i) \times 10^{-4},$$
$$\Gamma_{Z^* WW}(\sqrt{s} = 200\ \text{GeV}) = -(3.8 + 3.5i) \times 10^{-4},$$

that show similar order of magnitude values for the real part as in the $Z^* ZZ$ vertex but an enhanced absorptive part.

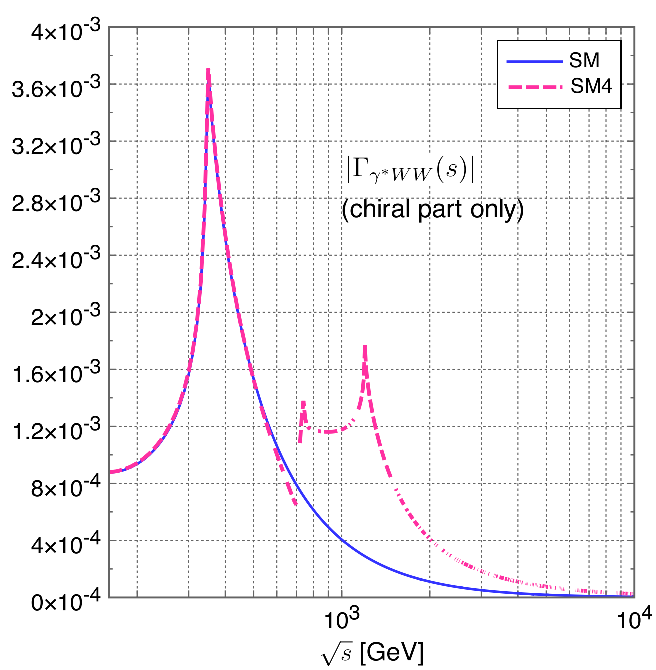

FIG. 5 (color online). The effective vertex $|\Gamma_{\gamma^* WW}(s)|$ in the minimal SM (solid line) and in SM with an extra fourth fermion generation (SM4), (dashed line).

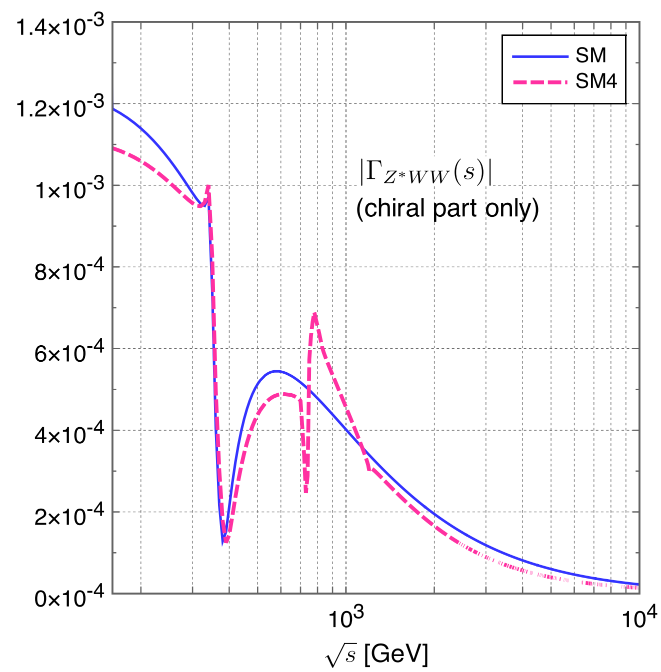

FIG. 6 (color online). The effective vertex $|\Gamma_{Z^* WW}(s)|$ in the minimal SM (solid line) and in SM with an extra fourth fermion generation (SM4), (dashed line).

The latter is due to custodial symmetry breaking effects i.e., the large mass difference between the top and the bottom quarks. Although there is an intense experimental ongoing analyses at LEP [63], Tevatron [64] and LHC [57,58] for the first three CP-invariant nonchiral operators, $f^V_{i=1...3}$ of Eq. (56), we are not aware of a similar experimental search on the chiral f^V_5 of Eq. (55).

B. Models with a sequential fourth fermion generation

In our first departure from the SM we assume a fourth generation matter of quarks and leptons. Apart from the fact that the 4th generation neutrino has to weight more than 45 GeV, a certain tuning to avoid EW constraints is needed. More specifically, one extra doublet of degenerate leptons contributes a piece of approximately $1/6\pi \approx 0.05$ into the S-parameter [65] while the current fit [66] to the EW data gives,

$$S = 0.04 \pm 0.10. \tag{65}$$

Therefore, a 4th, mass degenerate, fermion generation will contribute a $4/6\pi \approx 0.2$ piece to S-parameter which is incompatible with the fit. A certain mass difference or else a certain weak isospin violation is needed which is parameterized by the T parameter [65]. A consistent parameter space with EW precision data and published direct searches is

$$\begin{aligned} m_{\nu 4} &= 400\ \text{GeV}, \qquad m_{e4} = 660\ \text{GeV}, \\ m_{t4} &= 358\ \text{GeV}, \qquad m_{b4} = 372\ \text{GeV}. \end{aligned} \tag{66}$$

This mass spectrum corresponds to Tevatron experiments allowed region, where the analyses from CDF [67] have excluded t_4 and b_4 quarks to have masses smaller than the values quoted above.[8] The leptons mass spectrum is chosen such that it does not contribute significantly to the oblique parameters, e.g., for these values of lepton masses one has $\Delta S_l \simeq 0$ [66].

Because of the fact that the charges are the same as in the SM, the anomalies are canceled in each generation. It is important to notice here that if all the extra fermions were very heavy and had the same mass, no effect would be left back and the decoupling would work perfectly. The reason is, first of all, that the sum over all extra fermions of expressions that contain the finite integrals A_3, A_4 or A_5 vanishes because the integrand factors out a term $\sum_f c_f$, where c_f is the pre-anomaly factor of each fermion. But this sum is equal to zero for an anomaly-free generation. On the other hand, terms proportional to I_1 or I_2 in Eq. (4), in the limit of large fermion mass, are canceled exactly by the anomalous term for special values of w and z parameters that are fixed by the Bose symmetry in each case. But this constraint is not necessary, e.g., if an anomaly-free generation of very heavy mass degenerate chiral fermions is added to the SM, it has no effects at low energies, no matter what the values of w and z are. This is guaranteed by the fact that the extra generation is anomaly-free.

The numerical analysis for the three gauge bosons vertices is the same as previously. Using the approximate integral expressions from Appendix D, we draw plots for the amplitudes $|\Gamma_{V^*VV}(s)|$ and $|\Gamma_{V^*WW}(s)|$ versus $\sqrt{s}$ in different combinations of the external gauge bosons $V = \gamma$, Z. These plots are collected in Figs. 3, 5, and 6, respectively [dashed line].

The extra generation has a significant contribution to Γ's, in the region near twice the threshold of each extra fermion, where the amplitude rises until those values (shown as peaks in every combination of external gauge bosons) and drops fast as $1/s$ (apart from $V^*\gamma\gamma$ which drops as $1/s^2$). We see that for small values of energy the two curves (the curve that corresponds to the SM case and the curve that corresponds both to the SM and the 4th generation) have the same form. In this energetic region ($\sqrt{s} \lesssim 600$ GeV) the dominant feature is the first peak that corresponds to the threshold energy for the creation of the top quark ($\sqrt{s} \approx 350\ \text{GeV} \approx 2m_t$). In addition, the contribution from the extra fermionic generation is negligible, because all the extra fermions are heavy compared to the energy, i.e., ($2m_f > \sqrt{s}$). These extra fermions have more or less similar masses. As before with the top-quark mass, there is a cancellation between the anomaly contributions and the $I_{1,2}$ parts of the amplitude for each fermion separately. As a result, the total contribution from the fourth generation is negligible as we can see from Fig. 3.

The situation is different when $\sqrt{s}$ runs over the mass spectrum of the extra fermionic generation. Firstly for ($\sqrt{s} \gtrsim 600$ GeV) we see different peaks that correspond to the threshold energy for the creation of the extra fermions ($\sqrt{s} \approx 2m_i$). When ($2m_i < \sqrt{s} < 2m_j$), there is a nonzero contribution to the total amplitude. In this case, fermions whose masses are very heavy compared to $\sqrt{s}$, exhibit the same behavior as previously i.e., the anomalous term cancels out against the finite contribution.

Reading our results from Fig. 3, the best case for observing triple gauge boson vertex is $\gamma^*\gamma Z$ where $h_3^\gamma(\sqrt{s} = 500\ \text{GeV}) \approx 10^{-4}$. This is by 2 orders of magnitude below the expected LHC sensitivity (with $\Lambda \sim 1$ TeV) [40].

C. Minimal Z' models

Grand Unified Theories (GUTs) with rank larger than 4 could break to the SM gauge group times additional

[8] Currently, the sequential 4th generation is under siege from LHC [68]. If there exist new heavy SM type quarks, they will contribute a factor of up to $N_c^2 = 9$ into the Higgs production cross section for the (triangle) process $gg \to H$. The current cross section sensitivity at the LHC is within a few of the SM prediction and therefore it sets an indirect bound over the whole exclusion Higgs area, up to 550–600 GeV. Other direct bounds from the LHC on 4th generation top and bottom quarks involve assumptions about their mass difference to be smaller than the W-mass. These caveats are discussed in some detail with complete references in Ref. [69].

$U(1)$'s: $SU(3)\times SU(2)\times U(1)\times U(1)'^n$. This symmetry is broken down to $U(1)_{\rm em}$ and therefore there is a possibility of additional forces mediated by the Z' gauge bosons associated with the broken $U(1)'$ symmetries (for a review see Ref. [70]).

We shall concentrate here on minimal models with one additional neutral gauge boson, the Z'. Minimal here means models that contain no-additional i.e., no exotic, matter particles apart from the SM ones and right-handed neutrinos. The latter play a crucial role in cancelling anomalies due to the additional $U(1)'$ and in producing viably small neutrino masses. These models were devised first in Ref. [71] and later elaborated in Refs. [72,73]. Following the notation of [72] we can describe these models with three additional parameters: the mass of the new gauge boson, $M_{Z'}$, and the couplings g_Y and g_{BL}. The latter enter into the current which couples to the unmixed Z'_0 gauge boson as

$$J^\mu_{Z'_0}=\sum_{f=f_L,f_R}[g_YY_f+g_{BL}(B-L)_f]\bar f\gamma^\mu f. \tag{67}$$

From this, it is easy to construct $\mathcal{L}_{\rm int}$ in Eq. (24) with

$$\alpha^Z_f=\cos\theta'\alpha^{Z_0}_f-\sin\theta'\alpha^{Z'_0}_f, \tag{68a}$$

$$\alpha^{Z'}_f=\sin\theta'\alpha^{Z_0}_f+\cos\theta'\alpha^{Z'_0}_f, \tag{68b}$$

$$\beta^Z_f=\cos\theta'\beta^{Z_0}_f-\sin\theta'\beta^{Z'_0}_f, \tag{68c}$$

$$\beta^{Z'}_f=\sin\theta'\beta^{Z_0}_f+\cos\theta'\beta^{Z'_0}_f, \tag{68d}$$

where θ' is the mixing angle between Z and Z' gauge bosons given by,

$$\tan\theta'=-\frac{g_Y}{g_Z}\frac{M^2_{Z_0}}{M^2_{Z'}-M^2_{Z_0}}, \tag{69}$$

with $M^2_{Z_0}=g^2_Zv^2/4$ the "SM" Z-boson mass. Also in Eq. (68) we obtain for $\alpha^{Z'_0}_f$, $\beta^{Z'_0}_f$,

$$\begin{aligned}
\alpha^{Z'_0}_u&=\frac{1}{2}\Big(\frac{5}{6}g_Y+\frac{2}{3}g_{BL}\Big), & \beta^{Z'_0}_u&=\frac{g_Y}{4},\\
\alpha^{Z'_0}_d&=\frac{1}{2}\Big(-\frac{1}{6}g_Y+\frac{2}{3}g_{BL}\Big), & \beta^{Z'_0}_d&=-\frac{g_Y}{4},\\
\alpha^{Z'_0}_e&=\frac{1}{2}\Big(-\frac{3}{2}g_Y-2g_{BL}\Big), & \beta^{Z'_0}_e&=-\frac{g_Y}{4},\\
\alpha^{Z'_0}_\nu&=\frac{1}{2}\Big(-\frac{1}{2}g_Y-2g_{BL}\Big), & \beta^{Z'_0}_\nu&=\frac{g_Y}{4},
\end{aligned} \tag{70}$$

while the corresponding expressions for $\alpha^{Z_0}_f$, $\beta^{Z_0}_f$ are given by Eq. (26). This parameterization through g_Y and g_{BL} helps us to very easily incorporate several models that have been studied in the literature: Z_{B-L} when the $U(1)_{B-L}$ charges of the SM fermions are proportional to $(B-L)$ quantum numbers, Z_χ a GUT inspired $SO(10)\to SU(5)\times U(1)_\chi$ model and finally, Z_{3R} where the corresponding $U(1)_{3R}$ charges are proportional to T_{3R} generator of the global $SU(2)_R$ symmetry. We summarize the couplings of these models in the following table:

	Z_{B-L}	Z_χ	Z_{3R}
g_Y	0	$-\frac{2}{\sqrt{10}}g_{Z'}$	$-g_{Z'}$
g_{BL}	$\sqrt{\frac{3}{8}}g_{Z'}$	$\frac{5}{2\sqrt{10}}g_{Z'}$	$\frac{1}{2}g_{Z'}$

Here, we wish to calculate the effective vertices $\Gamma_{Z'^*\gamma Z}$ and $\Gamma_{Z'^*ZZ}$ for those models. Recalling Eqs. (38) and (27) with $i=Z'$, $j=\gamma$ or Z and $k=Z$ respectively, we obtain

$$\begin{aligned}
\Gamma^{\mu\nu\rho}_{Z'^*\gamma Z}(s)&\approx\epsilon^{\mu\nu\rho\sigma}k_{1\sigma}\sum_{f=u,d,e,\nu}\Big[m^2_Z(A_{3f}+A_{5f})-\frac{m^2_f\beta^Z_f}{\pi^2}I_{2f}\\
&\quad+\frac{(z+1)}{4\pi^2}(\alpha^{Z'}_f\beta^Z_f+\alpha^Z_f\beta^{Z'}_f)\alpha^\gamma_f\Big]\\
&\equiv\epsilon^{\mu\nu\rho\sigma}k_{1\sigma}\Gamma_{Z'^*\gamma Z}(s),
\end{aligned} \tag{71}$$

$$\begin{aligned}
\Gamma^{\mu\nu\rho}_{Z'^*ZZ}(s)&=\epsilon^{\mu\nu\rho\sigma}(k_1-k_2)_\sigma\sum_{f=u,d,e,\nu}\Big[m^2_Z(A_{3f}-A_{4f})\\
&\quad+\frac{m^2_f\beta^Z_f}{\pi^2}I_{1f}-\frac{(w-1)}{4\pi^2}[(\alpha^Z_f)^2\beta^{Z'}_f\\
&\quad+(\beta^Z_f)^2\beta^{Z'}_f+2\alpha^{Z'}_f\alpha^Z_f\beta^Z_f]\Big]\\
&\equiv\epsilon^{\mu\nu\rho\sigma}(k_1-k_2)_\sigma\Gamma_{Z'^*ZZ}(s),
\end{aligned} \tag{72}$$

with α_f, and β_f given in Eqs. (68) and (70). Again the last terms on the r.h.s of Eqs. (71) and (72) arrive from the chiral anomaly of individual fermion contributions. These anomalous terms cancel out when we sum over all SM fermions (here we also need the right-handed neutrino). This also removes the arbitrariness due to the unknown parameters w, z. Contrary to the SM vertices, we cannot use here any physical arguments in order to remove completely both w and z parameters. We only have $U(1)_{\rm em}$ gauge invariance for $Z'^*\gamma Z$ and Bose symmetry for Z'^*ZZ while in the SM we have two neutral gauge bosons and two symmetries.

But lets for the moment keep the anomalous terms. Obviously they are multiplied by arbitrary parameters $(z+1)$ (for $Z'^*\gamma Z$) and $(w-1)$ (for Z'^*ZZ). Focusing on the Z'_{B-L} model, where the mixing angle θ' vanishes, we observe that for any single heavy fermion contribution the 2nd and the 3rd term on the r.h.s of Eqs. (71) and (72) mutually cancel and what remains back is the effective theory with the low mass fermion contributions but *together with* their anomalous terms included. The latter do not depend on particle masses. The choices for the arbitrary parameters are $w=z=1$ for $Z'\gamma Z$ and $w=z=0$

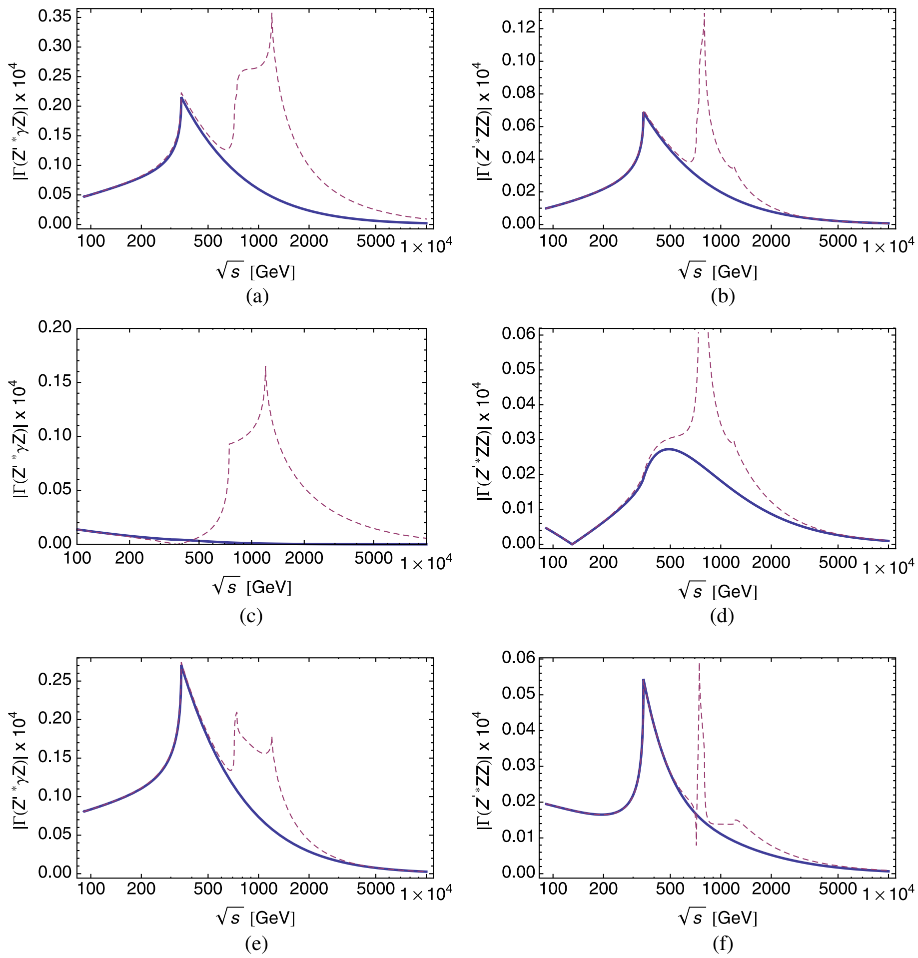

FIG. 7 (color online). a,b) $|\Gamma_{Z'VV}(s)|$ versus $\sqrt{s}$ for different gauge bosons combinations as they are given by Eqs. (71) and (72). The solid curve corresponds to the SM spectrum with an extra $U(1)_{B-L}$, while the dashed curve corresponds to the same but with a 4th sequential fermion generation added as in Fig. 3. We take $M_{Z'} = 1$ TeV and $g_{Z'} = \alpha_{\rm em}$. c,d) The same as (a,b) but with $U(1)_\chi$. (e, f) The same as (a,b) but with $U(1)_{3R}$.

for $Z'ZZ$. The last condition can be interpreted as follows: for the amplitude $ZZ \to ZZ$ to hold for asymptotic values of energies, Eq. (10) requires $w = z$ but Bose symmetry requires $w = -z$. This conclusion does not stand firm in the case of mixing between Z and Z' i.e., in models Z_χ, Z_{3R} of the table above, and the contribution of a heavy mass particle is undetermined. Of course anomalies do cancel when *all* model fermions are added.

In Fig. 7 we display numerical results for the absolute value of the scalar part of the 1PI effective vertices $Z'^*\gamma Z$ and Z'^*ZZ in Eqs. (71) and (72) for $M_{Z'} = 1$ TeV and $g_{Z'} = \alpha_{\rm em}$. Figures 7(a) and 7(b) refer to Z_{B-L} model, Figs. 7(c) and 7(d) to Z_χ models and, finally, Figs. 7(e) and 7(f) to Z_{3R} models. For the values of $M_{Z'}$ and $g_{Z'}$ chosen, fits to electroweak observables and direct searches are satisfied. We also present results when adding a sequential 4th generation of fermions with the same masses (and the reasoning) as we did for the SM case of section IVA. We observe that there is an enhancement of the vertices by a factor of 2 for Z_{B-L}, and a factor of 10–15 for Z_χ. Numerically, we can define analogous quantities $h_3^{Z'}$ and $f_5^{Z'}$ by simply replacing Z with Z' in the definition given by footnote 5. As an example, for the $B - L$ model we obtain,

$$\begin{aligned}
h_3^{Z'}(\sqrt{s} = 200\ \text{GeV}) &= -2.7 \times 10^{-5}, \\
h_3^{Z'}(\sqrt{s} = 500\ \text{GeV}) &= (-2.7 + 5.3i) \times 10^{-4}, \\
f_5^{Z'}(\sqrt{s} = 200\ \text{GeV}) &= -7.2 \times 10^{-6}, \\
f_5^{Z'}(\sqrt{s} = 500\ \text{GeV}) &= (-7.7 + 18i) \times 10^{-5}.
\end{aligned} \tag{73}$$

Numerical results for the vertices presented above and in Fig. 7 are based on various analytical approximations for form factors described in Appendix D.

Now that Z' can be heavy it is interesting to study its decay width into $Z\gamma$ and ZZ modes. Based on (1) and on Eqs. (71) and (72) the decay widths of the Z' can be read from

$$\Gamma(Z' \to \gamma Z) = \frac{1}{48\pi}\left|\sum_{f=u,d,e,\nu}\left[m_Z^2(A_{3f} + A_{5f}) - \frac{m_f^2\beta_f^Z}{\pi^2}I_{2f} + \frac{(z+1)}{4\pi^2}(\alpha_f^{Z'}\beta_f^Z + \alpha_f^Z\beta_f^{Z'})\alpha_f^\gamma\right]\right|^2 \times \frac{m_{Z'}^3}{m_Z^2}\left(1 - \frac{m_Z^2}{m_{Z'}^2}\right)^3\left(1 + \frac{m_Z^2}{m_{Z'}^2}\right), \tag{74}$$

$$\Gamma(Z' \to ZZ) = \frac{1}{96\pi}\left|\sum_{f=u,d,e,\nu}\left[m_Z^2(A_{3f} - A_{4f}) + \frac{m_f^2\beta_f^Z}{\pi^2}I_{1f} - \frac{(w-1)}{4\pi^2}[(\alpha_f^Z)^2\beta_f^{Z'} + (\beta_f^Z)^2\beta_f^{Z'} + 2\alpha_f^{Z'}\alpha_f^Z\beta_f^Z]\right]\right|^2 \frac{m_{Z'}^3}{m_Z^2}\left(1 - \frac{4m_Z^2}{m_{Z'}^2}\right)^{5/2}, \tag{75}$$

$$\Gamma(Z' \to W^+W^-) = \frac{\alpha_{\rm em} m_{Z'}\sin^2\theta'}{48\tan^2\theta_w}\left(1 - 4\frac{m_W^2}{m_{Z'}^2}\right)^{3/2} \times \left[1 + 20\frac{m_W^2}{m_{Z'}^2} + 12\frac{m_W^4}{m_{Z'}^4}\right]\left(\frac{m_W^2}{m_{Z'}^2}\right)^{-2}, \tag{76}$$

$$\Gamma(Z' \to \bar{f}f) = \frac{N_c m_{Z'}}{12\pi}\left[(\alpha_f^{Z'2} + \beta_f^{Z'2}) - \frac{3m_f^2}{m_{Z'}^2}(\alpha_f^{Z'2} - \beta_f^{Z'2})\right]\sqrt{1 - \frac{4m_f^2}{m_{Z'}^2}}, \tag{77}$$

where N_c is the color factor (3 for quarks and 1 for leptons) and the tree level decay width for $Z' \to WW$ has been taken from Ref. [74] and is dominant over the loop-induced ones. For $g_{Z'} = \alpha_{\rm em}$, $M_{Z'} = 1$ TeV and SM spectrum with three generations we obtain for the $B - L$ (χ) [$3R$] models:

$$\begin{aligned}
&\mathrm{Br}(Z' \to \nu\nu) = 37.7(42.3)[12.5]\%,\\
&\mathrm{Br}(Z' \to \ell\ell) = 37.7(12.5)[12.6]\%,\\
&\mathrm{Br}(Z' \to qq) = 24.5(45.1)[74.8]\%,\\
&\mathrm{Br}(Z' \to WW) = 0.03(3.2)[8.1] \times 10^{-5},\\
&\mathrm{Br}(Z' \to Z\gamma) = 5.8(\sim 10^{-3})[8.7] \times 10^{-6},\\
&\mathrm{Br}(Z' \to ZZ) = 3.0(2.5)[0.9] \times 10^{-7}.
\end{aligned} \tag{78}$$

These results are pretty much the same for bigger $M_{Z'}$ values. As we see, the branching fraction for $Z' \to \gamma Z$ is in the region of 10^{-5}–10^{-6} while for $Z' \to ZZ$ in the region $\sim 10^{-7}$. These are very challenging numbers even for LHC@14 TeV.

In coordinate space representation, the vertices (71) and (72) arise on-shell from the following operators

$$\mathcal{O}_{Z'\gamma Z} \sim \varepsilon^{\mu\nu\rho\sigma} Z'_\mu Z_\nu F_{\rho\sigma}, \tag{79}$$

$$\mathcal{O}_{Z'ZZ} \sim \varepsilon^{\mu\nu\rho\sigma} Z'_\mu Z_\nu \partial_\rho Z_\sigma, \tag{80}$$

which are both P-odd but CP-invariant. Although not present in the SM and in the Z'-models under consideration there may be P-even but CP-violating operators of the form $\mathcal{O}_{Z'ZZ} \sim Z'^\mu(\partial^\nu Z_\mu)Z_\nu$ induced by a triple scalar loop instead. The latter would interfere with (80) and there is a proposal in Ref. [75] on how their effects can be separated at the LHC. However, within minimal Z'-models considered here this looks very difficult due to tiny $\mathrm{Br}(Z' \to VV)$ of Eq. (78).

V. CONCLUSIONS

We construct an effective 1PI vertex for triple gauge bosons for every renormalized theory making explicit mentioning to the chiral anomalies and their synergy with heavy fermion decoupling phenomena. Our method for calculating the vertex is based on Ref. [38]. It is quite general and can be divided in four steps:

(1) Write down the most general, Lorentz (and/or possibly other symmetry) invariant effective vertex $\Gamma^{\mu\nu\rho}$ [like Eq. (2)] with unknown form factors.
(2) Isolate the -potentially- infinite form factors and calculate only the finite parts.
(3) Derive Ward Identities arising from the underlying spontaneously broken gauge symmetries at the quantum level. Apply them to $\Gamma^{\mu\nu\rho}$ and calculate the ambiguous form factors, thus forcing them to be finite.
(4) If the vertex is still undetermined i.e., if arbitrary parameters still remain, try to fix them by physical requirements. If nevertheless arbitrariness persists, then the model needs completion, perhaps with new particles or new dynamics.

This method, explained in detail in Appendix B and in Sec. II, does not require dimensional regularization or other integral regularization technics. It may require, however, "shifting momenta" technics like Eq. (B11). The above steps can be augmented with additional relations. Instead of WIs, one could use other identities like, for example, those arising from perturbative unitarity sum rules or the Goldstone boson equivalence theorem e.g., Eq. (11).

All the above steps are realized when calculating triple gauge boson vertices in spontaneously broken gauge theories, like, for example, the SM or its extensions like minimal Z'-models. The anomalous terms are arbitrary and can only be fixed by physics. Only then can we discuss nondecoupling effects in the broken limit. We observe that for V^*VV, $V = \gamma$, Z and for γ^*WW vertices, there are two arbitrary parameters that are completely determined by two physical symmetries: $U(1)_{\rm em}$ and Bose symmetry or CP-invariance. We find that at the limit of heavy fermion masses, nondecoupled terms cancel exactly those that arise from anomalies. For example, in the SM, decoupling of the top quark will leave behind anomalous-terms of light quarks and leptons plus finite parts. On the other hand vertices like Z^*WW, Z'^*VV are in general undetermined because there are no enough symmetries to fix the arbitrary parameters. Of course for anomaly-free models this arbitrariness is removed when adding up all fermion contributions.

We made a numerical analysis for SM and minimal Z'-model vertices. To this end, we made an effort to calculate finite integrals in terms of standard functions that are easy to handle. For example in Appendix D, we solved analytically the integrals for $V^*\gamma V$-vertices. We then proceeded to SM predictions for the triple gauge boson vertices. Unfortunately, it turns out that within the SM these are rather small to be discovered even at the LHC with $\sqrt{s} = 14$ TeV. Similar results are obtained in the SM extended by a sequential fourth fermion generation. The difference w.r.t the SM, is that $|\Gamma_{V^*VV}(s)|$ is "delayed" to vanish for large $\sqrt{s}$ due to the heavy, 4th generation thresholds (see Figs. 3). In the best case, the SM + 4th generation predicts a maximum of a few $\times 10^{-3}$ for $|\Gamma_{\gamma^*\gamma Z}|$ [see dashed lines in Figs. 3].

We have performed a numerical analysis, shown in Fig. 7, for minimal Z'-models with $U(1)_{B-L}$ symmetry, $SO(10)$-like and $U(1)_{3R}$ also extended with a 4th fermion generation. For a conservative choice of $M_{Z'} = 1$ TeV and $g_Z = \alpha_{\rm em}$, we find $|\Gamma_{Z'ZZ}|$ and $|\Gamma_{Z'\gamma Z}|$ in the regime below a few $\times 10^{-5}$. We also briefly discussed Z'-decays to $Z\gamma$ and ZZ. Adopting the parameters space above, their branching ratio come out to be in the neighborhood of $\sim 10^{-5}$ and $\sim 10^{-7}$, respectively.

In Sec. III B and Appendix E, we calculated nondecoupling effects that arise instantaneously with vanishing anomalies. We constructed several toy models with two or three external gauge bosons and a number of fermions where this situation could take place. In principle, these models can be used as a basis towards realistic extensions of the SM.

Our main result, the effective triple gauge boson vertex obtained in section II can be used in various ways: i) in models with anomalous spectrum, ii) in realistic anomaly driven models of Sec. III B, iii) in MSSM and its extensions, iv) in dark matter or neutrino—nucleon scattering processes with a photon in the final state. We will pursue some of these issues in a forthcoming article.

ACKNOWLEDGMENTS

We would like to thank I. Antoniadis, H. Haber, P. Kanti, S. Martin, A. Pilaftsis, and K. Tamvakis for useful discussions. This research Project is cofinanced by the European Union—European Social Fund (ESF) and National Sources, in the framework of the program THALIS of the "Operational Program Education and Lifelong Learning" of the National Strategic Reference Framework (NSRF) 2007-2013. K. S. acknowledges full financial support from Greek State Scholarships Foundation (I. K. Y).

APPENDIX A: A SET-UP TOY MODEL FOR CALCULATIONS

Consider a gauge theory of a complex scalar field Φ charged under a local $U(1)$ with charge Y_Φ (in units of e), a vector spin-1 abelian gauge boson A_μ and a pair of Dirac fermions E_L and e_R with $U(1)$-charges Y_L and Y_R respectively. This gauge theory is described by the Lagrangian,[9]

$$\mathcal{L} = \mathcal{L}_g(\Phi, A_\mu) + \mathcal{L}_f(E_L, e_R, A_\mu) + \mathcal{L}_Y(E_L, e_R, \Phi), \tag{A1}$$

where the gauge boson-scalar interactions are

$$\mathcal{L}_g(\Phi, A_\mu) = -\frac{1}{4}F_{\mu\nu}F^{\mu\nu} - \frac{1}{2}(G)^2 + |D_\mu\Phi|^2 - V(\Phi), \tag{A2}$$

while the chiral fermion and the Yukawa interaction parts of the Lagrangian in Eq. (A1) are stored in

$$\mathcal{L}_f(E_L, e_R, A_\mu) = \bar{E}_L(i\not{D})E_L + \bar{e}_R(i\not{D})e_R, \tag{A3}$$

$$\mathcal{L}_Y(E_L, e_R, \Phi) = -\lambda_e(\bar{E}_L\Phi e_R + \bar{e}_R\Phi^* E_L), \tag{A4}$$

and $D_\mu\Phi = \partial_\mu\Phi + ieY_\Phi A_\mu\Phi$, $D_\mu E_L = \partial_\mu E_L + ieY_L A_\mu E_L$, and $D_\mu e_R = \partial_\mu e_R + ieY_R A_\mu e_R$. $\mathcal{L}_g$ is invariant under the local, $U(1)$ gauge-transformation

$$\Phi(x) \to e^{ieY_\Phi\Lambda(x)}\Phi(x), \qquad A_\mu(x) \to A_\mu(x) - \partial_\mu\Lambda(x), \tag{A5}$$

$$E_L(x) \to e^{ieY_L\Lambda(x)}E_L(x), \qquad e_R(x) \to e^{ieY_R\Lambda(x)}e_R(x), \tag{A6}$$

iff $Y_\Phi = Y_L - Y_R$. It is convenient to combine the left and right-handed fermions into a single Dirac four-component spinor $\Psi = (E_L, e_R)^T$. Then the interaction Lagrangian relevant to our study for triangle graphs reads:

$$\begin{aligned}\mathcal{L}_{\rm int} = &-\lambda_e\bar{\Psi}\Phi P_R\Psi - \lambda_e\bar{\Psi}\Phi^* P_L\Psi \\ &- eA_\mu\bar{\Psi}\gamma^\mu(\alpha + \beta\gamma_5)\Psi,\end{aligned} \tag{A7}$$

where

$$\alpha = \frac{Y_L + Y_R}{2}, \qquad \beta = \frac{Y_R - Y_L}{2}. \tag{A8}$$

Under gauge transformations the 4-component field Ψ transforms as

$$\Psi(x) \to e^{ie(\alpha+\beta\gamma_5)\Lambda(x)}\Psi(x), \tag{A9a}$$

$$\bar{\Psi}(x) \to \bar{\Psi}(x)e^{-ie(\alpha-\beta\gamma_5)\Lambda(x)}, \tag{A9b}$$

which together with Eq. (A6) leave $\mathcal{L}$ invariant if $Y_\Phi = -2\beta$.

[9] Throughout we follow the notation and conventions of Ref. [76].

We choose a renormalizable and gauge invariant potential $V(\Phi)$ such that the field Φ acquires a nonvanishing vacuum expectation value, $\langle\Phi\rangle = v/\sqrt{2}$, which breaks the local $U(1)$ symmetry spontaneously. We expand Eq. (A1) around the minimum, $\Phi = \frac{1}{\sqrt{2}}(v + h + i\varphi)$ and choose a gauge-fixing function in Eq. (A2),

$$G = \frac{1}{\sqrt{\xi}}(\partial_\mu A^\mu - \xi e v \varphi), \tag{A10}$$

which eliminates the Goldstone boson—gauge boson mixing term. The mass of the vector boson A_μ and of the unphysical Goldstone boson φ in this R_ξ-gauge become

$$m_A = evY_\Phi, \qquad m_\varphi^2 = \xi m_A^2. \tag{A11}$$

The ghost part of $\mathcal{L}$ is not relevant to our discussion for the one-loop triangle graphs and is not presented. In terms of Ψ and $\bar{\Psi}$, $\mathcal{L}_f + \mathcal{L}_Y$ becomes

$$\begin{aligned}\mathcal{L}_f(\Psi, A_\mu) + \mathcal{L}_Y(\Psi, h, \varphi) = {} & \bar{\Psi} i\not{\partial}\Psi - eA_\mu \bar{\Psi}\gamma^\mu \\ & \times (\alpha + \beta\gamma^5)\Psi - m\bar{\Psi}\Psi \\ & - \tilde{\beta}\bar{\Psi}h\Psi - i\tilde{\beta}\bar{\Psi}\gamma^5\varphi\Psi,\end{aligned} \tag{A12}$$

where $m = v\tilde{\beta}$ and $\tilde{\beta} = \frac{\lambda_e}{\sqrt{2}}$.

This model, albeit very simple, captures the most important nondecoupling heavy fermion effects in the trilinear gauge boson vertices in the SM and its extensions. In the context of chiral anomalies it has been exploited in Ref. [15]. With a light language deform it imitates the Standard Model with the difference that its WI's for the currents corresponding to the gauge symmetry in Eq. (A6) are anomalous as we shall see below.

APPENDIX B: CALCULATION OF THE THREE POINT GAUGE BOSON VERTEX

In this Appendix we explicitly evaluate the three external gauge boson, fermionic one-loop amplitude of Fig. 1. The loop function is calculated directly in four dimensions using standard methods studied in Refs. [7,38,77–79]. Here, we review this calculation in detail for the toy model of Appendix A. At the end we generalize our results to the case of three different external (massive or massless) gauge bosons.

By naive power counting we observe that the two diagrams in Fig. 1 are linearly divergent. This means that their quantum amplitudes depend on the routing of the internal momenta circulating in the loop. In each of the two diagrams we shift the internal momenta with arbitrary four vectors a^μ and b^μ, respectively. By reading Feynman rules from Eq. (A7), the graphs in Fig. 1 become

$$\begin{aligned}\Gamma^{\mu\nu\rho}(k_1, k_2; a, b) = {} & (-1)e^3\,\mathrm{Tr}\Bigg\{\int \frac{d^4p}{(2\pi)^4} \\ & \times \frac{\gamma^\mu(\alpha+\beta\gamma^5)(\not{p} - \not{k}_2 + \not{a} + m)\gamma^\rho(\alpha+\beta\gamma^5)(\not{p} + \not{a} + m)\gamma^\nu(\alpha+\beta\gamma^5)(\not{p} + \not{k}_1 + \not{a} + m)}{[(p-k_2+a)^2 - m^2][(p+a)^2 - m^2][(p+k_1+a)^2 - m^2]} \\ & + \int \frac{d^4p}{(2\pi)^4}\frac{\gamma^\mu(\alpha+\beta\gamma^5)(\not{p} - \not{k}_1 + \not{b} + m)\gamma^\nu(\alpha+\beta\gamma^5)(\not{p} + \not{b} + m)\gamma^\rho(\alpha+\beta\gamma^5)(\not{p} + \not{k}_2 + \not{b} + m)}{[(p-k_1+b)^2 - m^2][(p+b)^2 - m^2][(p+k_2+b)^2 - m^2]}\Bigg\},\end{aligned} \tag{B1}$$

where m is the fermion mass and (-1) is a fermionic loop factor. The integral in the second line is the same as the first with only the difference that the upper two external legs in Fig. 1 are interchanged, i.e., $\{\nu, \rho\} \leftrightarrow \{\rho, \nu\}$ and $k_1 \leftrightarrow k_2$. Dimensional regularization is a scheme not well suited in calculating (B1) due to the problems in defining γ_5 and $\epsilon^{\mu\nu\rho\sigma}$ in $d > 4$ spacetime dimensions. We here follow a method for calculating (B1) first presented by Rosenberg in Ref. [38] and later used by Adler in his classic paper on chiral anomaly [7]. Basically, this method relies on the fact that the ambiguous part of the integral is stored in two form factors in $\Gamma^{\mu\nu\rho}$ expansion, A_2 and A_1, that multiply the external momenta k_1 and k_2, respectively. We then exploit physical arguments like, for example, conservation of charge, in order to determine the form factors A_1, A_2—all others, $A_3 \ldots A_6$ are finite and can be calculated directly in 4-dimensions.

Our next step is to write down the WIs. This can be done in many ways, probably the most insightful is the use of functional methods (see for instance Chapter 9.6 in the textbook of Ref. [76]). One finds the classical WIs of Eq. (3), but not the last term on the r.h.s. We show below how to calculate this last term. We need first to calculate the divergence of the 1PI vertex: $q_\mu\Gamma^{\mu\nu\rho} = (k_1 + k_2)_\mu\Gamma^{\mu\nu\rho}$. It is useful to employ the following algebraic identity:

$$\begin{aligned}\not{q}(\alpha+\beta\gamma^5) = {} & -(\alpha - \beta\gamma^5)(\not{p} - \not{k}_2 + \not{a} - m) + 2\beta\gamma^5 m \\ & + (\not{p} + \not{k}_1 + \not{a} - m)(\alpha + \beta\gamma^5),\end{aligned} \tag{B2}$$

in the first integral of (B1) and a similar identity with $a \to b$ and $k_1 \to k_2$ in the second one. These identities split $q_\mu\Gamma^{\mu\nu\rho}$ into two parts,

$$q_\mu \Gamma^{\mu\nu\rho}(k_1, k_2; a, b) = -\frac{2m\beta ei}{\tilde{\beta}} \Gamma^{\nu\rho}(k_1, k_2; a, b) + \Pi^{\nu\rho}(k_1, k_2; a, b), \tag{B3}$$

a part that is proportional to the fermion mass m and a part which contains divergent two-point functions that *would had been zero if shifting of the momenta variable was allowed*. The latter integrals will be responsible for the failure of the axial vector WI's. Explicitly $\Gamma^{\rho\nu}$ and $\Pi^{\rho\nu}$ in Eq. (B3) read,

$$\begin{aligned}\Gamma^{\nu\rho}(k_1, k_2; a, b) &= -ie^2\tilde{\beta}\,\mathrm{Tr}\bigg\{\int \frac{d^4p}{(2\pi)^4} \frac{\gamma^5(\not{p} - \not{k}_2 + \not{a} + m)\gamma^\rho(\alpha + \beta\gamma^5)(\not{p} + \not{a} + m)\gamma^\nu(\alpha + \beta\gamma^5)(\not{p} + \not{k}_1 + \not{a} + m)}{[(p - k_2 + a)^2 - m^2][(p + a)^2 - m^2][(p + k_1 + a)^2 - m^2]} \\ &\quad + \int \frac{d^4p}{(2\pi)^4} \frac{\gamma^5(\not{p} - \not{k}_1 + \not{b} + m)\gamma^\nu(\alpha + \beta\gamma^5)(\not{p} + \not{b} + m)\gamma^\rho(\alpha + \beta\gamma^5)(\not{p} + \not{k}_2 + \not{b} + m)}{[(p - k_1 + b)^2 - m^2][(p + b)^2 - m^2][(p + k_2 + b)^2 - m^2]}\bigg\} \\ &= \frac{-ie^2m\tilde{\beta}}{2\pi^2} \varepsilon^{\lambda\nu\rho\sigma} k_{1\lambda} k_{2\sigma} I_0(k_1, k_2, m),\end{aligned} \tag{B4}$$

where

$$I_0(k_1, k_2, m) = \int_0^1 dx \int_0^{1-x} dy \frac{(\alpha^2 - \beta^2) + 2(x + y)\beta^2}{x(x - 1)k_2^2 + y(y - 1)k_1^2 - 2xyk_1 \cdot k_2 + m^2}. \tag{B5}$$

Obviously, the integral in $\Gamma^{\nu\rho}$ in Eq. (B4) is obtained from $\Gamma^{\mu\nu\rho}$ in Eq. (B1) with the replacement $\gamma^\mu(\alpha + \beta\gamma^5) \longrightarrow \gamma^5$, that is a replacement of a vector-axial vector coupling with a pseudoscalar. This validates the PCAC relation in Eq. (B3). Note that $\Gamma^{\nu\rho}$ is finite and independent on the arbitrary vectors a^μ and b^μ: $\Gamma^{\nu\rho}(k_1, k_2; a, b) = \Gamma^{\nu\rho}(k_1, k_2)$.

The divergent part $\Pi^{\nu\rho}$ in the WI of Eq. (B3) contains, among others, the anomalous term. It is written explicitly as,

$$\begin{aligned}\Pi^{\nu\rho}(k_1, k_2; a, b) &= (-e^3)\,\mathrm{Tr}\int \frac{d^4p}{(2\pi)^4}\bigg\{-\frac{(\alpha - \beta\gamma^5)(\alpha - \beta\gamma^5)\gamma^\rho(\not{p} + \not{a} + m)\gamma^\nu(\alpha + \beta\gamma^5)(\not{p} + \not{k}_1 + \not{a} + m)}{[(p + a)^2 - m^2][(p + k_1 + a)^2 - m^2]} \\ &\quad + \frac{(\not{p} - \not{k}_2 + \not{a} + m)\gamma^\rho(\alpha + \beta\gamma^5)(\not{p} + \not{a} + m)\gamma^\nu(\alpha + \beta\gamma^5)(\alpha + \beta\gamma^5)}{[(p + a)^2 - m^2][(p - k_2 + a)^2 - m^2]} \\ &\quad - \frac{(\alpha - \beta\gamma^5)(\alpha - \beta\gamma^5)\gamma^\nu(\not{p} + \not{b} + m)\gamma^\rho(\alpha + \beta\gamma^5)(\not{p} + \not{k}_2 + \not{b} + m)}{[(p + b)^2 - m^2][(p + k_2 + b)^2 - m^2]} \\ &\quad + \frac{(\not{p} - \not{k}_1 + \not{b} + m)\gamma^\nu(\alpha + \beta\gamma^5)(\not{p} + \not{b} + m)\gamma^\rho(\alpha + \beta\gamma^5)(\alpha + \beta\gamma^5)}{[(p + b)^2 - m^2][(p - k_1 + b)^2 - m^2]}\bigg\}.\end{aligned} \tag{B6}$$

This is an integral that is divided into two parts: a chiral expression i.e., the one that contains γ^5 and a nonchiral expression that does not contain γ^5. Since the anomalous term is originated from the chiral part we start from there. Hence,

$$\begin{aligned}\Pi^{\nu\rho}_{\mathrm{chiral}}(k_1, k_2; a, b) &= (\beta^3 + 3\alpha^2\beta)e^3\,\mathrm{Tr}\int \frac{d^4p}{(2\pi)^4}\bigg\{\frac{(\not{p} + \not{k}_1 + \not{a})\gamma^\rho(\not{p} + \not{a})\gamma^\nu\gamma^5}{[(p + k_1 + a)^2 - m^2][(p + a)^2 - m^2]} \\ &\quad - \frac{(\not{p} + \not{a})\gamma^\nu(\not{p} - \not{k}_2 + \not{a})\gamma^\rho\gamma^5}{[(p + a)^2 - m^2][(p - k_2 + a)^2 - m^2]} + \frac{(\not{p} + \not{k}_2 + \not{b})\gamma^\nu(\not{p} + \not{b})\gamma^\rho\gamma^5}{[(p + k_2 + b)^2 - m^2][(p + b)^2 - m^2]} \\ &\quad - \frac{(\not{p} + \not{b})\gamma^\rho(\not{p} - \not{k}_1 + \not{b})\gamma^\nu\gamma^5}{[(p + b)^2 - m^2][(p - k_1 + b)^2 - m^2]}\bigg\}.\end{aligned} \tag{B7}$$

Grouping together the first and the fourth as well as the third and the second terms in the integrand of Eq. (B7), we arrive at,

$$\begin{aligned}\Pi^{\nu\rho}_{\mathrm{chiral}}(k_1, k_2; a, b) &= (\beta^3 + 3\alpha^2\beta)e^3 \int \frac{d^4p}{(2\pi)^4}\bigg\{\mathrm{Tr}(\gamma^\kappa\gamma^\rho\gamma^\lambda\gamma^\nu\gamma^5)\bigg(\frac{(p + k_1 + a)_\kappa(p + a)_\lambda}{[(p + k_1 + a)^2 - m^2][(p + a)^2 - m^2]} \\ &\quad - \frac{(p + b)_\kappa(p - k_1 + b)_\lambda}{[(p + b)^2 - m^2][(p - k_1 + b)^2 - m^2]}\bigg) + \mathrm{Tr}(\gamma^\kappa\gamma^\nu\gamma^\lambda\gamma^\rho\gamma^5) \\ &\quad \times\bigg(\frac{(p + k_2 + b)_\kappa(p + b)_\lambda}{[(p + k_2 + b)^2 - m^2][(p + b)^2 - m^2]} - \frac{(p + a)_\kappa(p - k_2 + a)_\lambda}{[(p + a)^2 - m^2][(p - k_2 + a)^2 - m^2]}\bigg)\bigg\}.\end{aligned} \tag{B8}$$

Following the steps described in Ref. [78], we first define a function and an integral,

$$f_{\kappa\lambda}(p;c,d)=\frac{(p+c)_\kappa(p+d)_\lambda}{[(p+c)^2-m^2][(p+d)^2-m^2]}, \quad \text{(B9)}$$

and

$$I_{\kappa\lambda}(k;c,d)=\int\frac{d^4p}{(2\pi)^4}[f_{\kappa\lambda}(p+k;c,d)-f_{\kappa\lambda}(p;c,d)], \quad \text{(B10)}$$

where c, d are arbitrary four vectors. By exploiting the following "momentum shift" integral relation (see the lecture by R. Jackiw in Ref. [77] and Refs. [48,49,79])

$$\int\frac{d^4p}{(2\pi)^4}[f(p+a)-f(p)]=\frac{i}{(2\pi)^4}\Big[2\pi^2 a_\mu\lim_{p\to\infty}p^\mu p^2 f_o(p) + \pi^2 a_\mu a_\nu\lim_{p\to\infty}p^\mu p^2\frac{\partial f_e(p)}{\partial p_\nu}\Big], \quad \text{(B11)}$$

where only the first term on the r.h.s is relevant to linearly divergent diagrams, and,

$$f_o(p)=\frac{1}{2}[f(p)-f(-p)],\qquad f_e(p)=\frac{1}{2}[f(p)+f(-p)], \quad \text{(B12)}$$

are the odd and even parts of $f(p)$ respectively, we obtain,[10]

$$I_{\kappa\lambda}(k;c,d)=\frac{i}{96\pi^2}[2k_\lambda c_\kappa+2k_\kappa d_\lambda-k_\lambda d_\kappa-k_\kappa c_\lambda - g_{\kappa\lambda}k\cdot(k+c+d)+k_\lambda k_\kappa]. \quad \text{(B13)}$$

Now we have all the necessary machinery to calculate $\Pi^{\nu\rho}$ in Eq. (B8) by applying to it Eqs. (B11) and (B13). For the nonchiral part of $\Pi^{\nu\rho}$ the choice $b=-a$ results in $\Pi^{\nu\rho}_{\text{non-chiral}}=0$ as we expect, since there should be *no* nonchiral anomalies. With this assignment for vector b we finally obtain for the chiral part:

$$\Pi^{\nu\rho}_{\text{chiral}}(k_1,k_2;a,-a)=\frac{e^3(\beta^3+3\alpha^2\beta)}{4\pi^2}\varepsilon^{\kappa\nu\lambda\rho}a_\kappa(k_1+k_2)_\lambda. \quad \text{(B14)}$$

Plugging in Eqs. (B4) and (B14) into Eq. (B3), the WI associated to the leg—μ—becomes:

$$q_\mu\Gamma^{\mu\nu\rho}(k_1,k_2;a,-a)=-\frac{2me\beta i}{\tilde\beta}\Gamma^{\nu\rho}(k_1,k_2)+\frac{e^3(\beta^3+3\alpha^2\beta)}{4\pi^2}\times\varepsilon^{\kappa\nu\lambda\rho}a_\kappa(k_1+k_2)_\lambda. \quad \text{(B15)}$$

[10] There is a typographical error in the corresponding expression of a classic textbook written by S. Weinberg in Ref. [78]. We thank Steve Martin and Howie Haber for communication related to this point.

Along the same lines we can build in the WIs for the other vertices. For example, the WI referring to the conservation of current in vertex—ν—(see Fig. 1) reads:

$$-k_{1\nu}\tilde\Gamma^{\nu\rho\mu}(k_1,k_2;a,-a)=-\frac{2m\beta ei}{\tilde\beta}\tilde\Gamma^{\rho\mu}(k_1,k_2)-\frac{e^3(\beta^3+3\alpha^2\beta)}{4\pi^2}\times\varepsilon^{\kappa\rho\lambda\mu}(a-k_2)_\kappa k_{1\lambda}. \quad \text{(B16)}$$

Vertices $\tilde\Gamma^{\nu\rho\mu}(k_1,k_2;a,b)$ and $\tilde\Gamma^{\rho\mu}(k_1,k_2)$ are obtained from $\Gamma^{\mu\nu\rho}(k_1,k_2;a,b)$ and $\Gamma^{\nu\rho}(k_1,k_2)$ in Eqs. (B1) and (B4), respectively, after the following replacements

$$\begin{aligned}&\mu\to\nu,\qquad \nu\to\rho,\qquad \rho\to\mu,\qquad a\to a-k_2,\\ &b\to b+k_2,\qquad k_1\to k_2,\qquad k_2\to -k_1-k_2,\\ &q=k_1+k_2\to k_2-k_1-k_2=-k_1\Rightarrow q\to -k_1.\end{aligned} \quad \text{(B17)}$$

It is straightforward to see from Eq. (B17) that the nonchiral part of $-k_{1\nu}\tilde\Gamma^{\nu\rho\mu}(k_1,k_2;a,b)$ vanishes again for the choice $b=-a$. Similarly the WI for the current conservation in the—ρ—vertex,

$$-k_{2\rho}\hat\Gamma^{\rho\mu\nu}(k_1,k_2;a,-a)=-\frac{2m\beta ei}{\tilde\beta}\hat\Gamma^{\mu\nu}(k_1,k_2)-\frac{e^3(\beta^3+3\alpha^2\beta)}{4\pi^2}\times\varepsilon^{\kappa\mu\lambda\nu}(a+k_1)_\kappa k_{2\lambda}. \quad \text{(B18)}$$

As previously, $\hat\Gamma^{\rho\mu\nu}(k_1,k_2;a,b)$ and $\hat\Gamma^{\mu\nu}(k_1,k_2)$ can be obtained from Eqs. (B1) and (B4) by making the following replacements:

$$\begin{aligned}&\mu\to\rho,\qquad \nu\to\mu,\qquad \rho\to\nu,\qquad a\to a+k_1,\\ &b\to b-k_1,\qquad k_1\to -k_2-k_1,\qquad k_2\to k_1,\\ &q=k_1+k_2\to -k_2-k_1+k_1\Rightarrow q\to -k_2.\end{aligned} \quad \text{(B19)}$$

These replacements leave invariant the choice $b=-a$ so that finally, the nonchiral part of $-k_{2\rho}\hat\Gamma^{\rho\mu\nu}(k_1,k_2;a,-a)$ vanishes identically everywhere. Furthermore, by direct calculation the vertices $\tilde\Gamma^{\rho\mu}$ and $\hat\Gamma^{\mu\nu}$ are found to be,

$$\tilde\Gamma^{\rho\mu}(k_1,k_2)=\frac{ie^2m\tilde\beta}{2\pi^2}\varepsilon^{\lambda\mu\xi\rho}k_{1\lambda}k_{2\xi}I_1(k_1,k_2,m), \quad \text{(B20)}$$

and

$$\hat\Gamma^{\mu\nu}(k_1,k_2)=\frac{ie^2m\tilde\beta}{2\pi^2}\varepsilon^{\lambda\mu\xi\nu}k_{1\lambda}k_{2\xi}I_2(k_1,k_2,m), \quad \text{(B21)}$$

respectively, where the corresponding integrals $I_{1,2}$ are written explicitly as,

$$I_1(k_1,k_2,m)=\int_0^1 dx\int_0^{1-x} dy\frac{-(\alpha^2+\beta^2)+2x\beta^2}{x(x-1)k_2^2+y(y-1)k_1^2-2xyk_1\cdot k_2+m^2}, \tag{B22}$$

and

$$I_2(k_1,k_2,m)=\int_0^1 dx\int_0^{1-x} dy\frac{(\alpha^2+\beta^2)-2y\beta^2}{x(x-1)k_2^2+y(y-1)k_1^2-2xyk_1\cdot k_2+m^2}. \tag{B23}$$

The three-point vertex obeys the following equality,

$$\Gamma^{\mu\nu\rho}=\tilde{\Gamma}^{\nu\rho\mu}=\hat{\Gamma}^{\rho\mu\nu}, \tag{B24}$$

as the property of trace to remain invariant under cyclic permutations. It is instructive to write the arbitrary vector a^μ, appearing in the WIs, as a linear combination of the two independent momenta k_1 and k_2,

$$a^\mu=zk_1^\mu+wk_2^\mu, \tag{B25}$$

with z, w arbitrary real numbers. Then the WIs in Eqs. (B15), (B16), and (B18) can be written explicitly in terms of the three integrals I_0, I_1, and I_2 and the real numbers w and z as,

$$q_\mu\Gamma^{\mu\nu\rho}(k_1,k_2;w,z)=-\frac{e^3\beta m^2}{\pi^2}\varepsilon^{\lambda\nu\rho\sigma}k_{1\lambda}k_{2\sigma}I_0(k_1,k_2;m)+\frac{e^3(\beta^3+3\alpha^2\beta)}{4\pi^2}\varepsilon^{\lambda\nu\rho\sigma}k_{1\lambda}k_{2\sigma}(w-z). \tag{B26}$$

$$-k_{1\nu}\tilde{\Gamma}^{\nu\rho\mu}(k_1,k_2;w)=-\frac{e^3\beta m^2}{\pi^2}\varepsilon^{\lambda\mu\rho\sigma}k_{1\lambda}k_{2\sigma}I_1(k_1,k_2;m)+\frac{e^3(\beta^3+3\alpha^2\beta)}{4\pi^2}\times\varepsilon^{\lambda\mu\rho\sigma}(w-1)k_{1\lambda}k_{2\sigma}, \tag{B27}$$

$$-k_{2\rho}\hat{\Gamma}^{\rho\mu\nu}(k_1,k_2;z)=-\frac{e^3\beta m^2}{\pi^2}\varepsilon^{\lambda\mu\nu\sigma}k_{1\lambda}k_{2\sigma}I_2(k_1,k_2;m)+\frac{e^3(\beta^3+3\alpha^2\beta)}{4\pi^2}\varepsilon^{\lambda\mu\nu\sigma}(z+1)k_{1\lambda}k_{2\sigma}. \tag{B28}$$

Obviously, even if we choose $w=1$ and $z=-1$ so that the second and third anomalous terms vanish it cannot be done so for the first one. The second term on the r.h.s of Eq. (B26), remains. It is quite interesting to note that in the limit where k_1^2, k_2^2, $k_1\cdot k_2\ll m\to\infty$, there is a choice for $w=-z=1/3$ such that the right hand side of Eqs. (B26)–(B28) vanishes identically. For this choice the fermions get decoupled completely.

Our goal is still to calculate the three gauge boson vertex $\Gamma^{\mu\nu\rho}(k_1,k_2;a,-a)$. The idea is to first write down the most general, Lorentz invariant vertex, as[11]

$$\begin{aligned}\Gamma^{\mu\nu\rho}(k_1,k_2;a,-a)=[&A_1(k_1,k_2;a,-a)\varepsilon^{\mu\nu\rho\sigma}k_{2\sigma}+A_2(k_1,k_2;a,-a)\varepsilon^{\mu\nu\rho\sigma}k_{1\sigma}+A_3(k_1,k_2)\varepsilon^{\mu\rho\beta\delta}k_2^\nu k_{1\beta}k_{2\delta}\\&+A_4(k_1,k_2)\varepsilon^{\mu\rho\beta\delta}k_1^\nu k_{1\beta}k_{2\delta}+A_5(k_1,k_2)\varepsilon^{\mu\nu\beta\delta}k_2^\rho k_{1\beta}k_{2\delta}+A_6(k_1,k_2)\varepsilon^{\mu\nu\beta\delta}k_1^\rho k_{1\beta}k_{2\delta}].\end{aligned} \tag{B32}$$

The form factors A_1 and A_2 are dimensionless and, by naive power counting, at most linearly divergent while all the rest, $A_3\dots A_6$ possess dimension of m^{-2} and are finite. The latter can be calculated directly in four dimensions from Eq. (B1). We find explicitly:

$$A_3(k_1,k_2)=-A_6(k_1,k_2)=-\frac{e^3(\beta^3+3\alpha^2\beta)}{\pi^2}\int_0^1 dx\int_0^{1-x}dy\frac{xy}{\Delta}, \tag{B33}$$

$$A_4(k_1,k_2)=\frac{e^3(\beta^3+3\alpha^2\beta)}{\pi^2}\int_0^1 dx\int_0^{1-x}dy\frac{y(y-1)}{\Delta}, \tag{B34}$$

[11]There are two more terms allowed in the expansion,

$$A_7(k_1,k_2)\varepsilon^{\rho\nu\beta\delta}k_2^\mu k_{1\beta}k_{2\delta}+A_8(k_1,k_2)\varepsilon^{\rho\nu\beta\delta}k_1^\mu k_{1\beta}k_{2\delta}. \tag{B29}$$

However, by exploiting the following, very useful, identities

$$k_1^\mu\varepsilon^{\rho\nu\beta\delta}k_{1\beta}k_{2\delta}=-\varepsilon^{\mu\rho\beta\delta}k_1^\nu k_{1\beta}k_{2\delta}+\varepsilon^{\mu\nu\beta\delta}k_1^\rho k_{1\beta}k_{2\delta}+\varepsilon^{\mu\nu\rho\alpha}[(k_1\cdot k_2)k_{1\alpha}-k_1^2k_{2\alpha}], \tag{B30}$$

$$k_2^\mu\varepsilon^{\rho\nu\beta\delta}k_{1\beta}k_{2\delta}=-\varepsilon^{\mu\rho\beta\delta}k_2^\nu k_{1\beta}k_{2\delta}+\varepsilon^{\mu\nu\beta\delta}k_2^\rho k_{1\beta}k_{2\delta}-\varepsilon^{\mu\nu\rho\alpha}[(k_1\cdot k_2)k_{2\alpha}-k_2^2k_{1\alpha}], \tag{B31}$$

we arrive at the six form factors given in Eq. (B32).

$$A_5(k_1, k_2) = -\frac{e^3(\beta^3 + 3\alpha^2\beta)}{\pi^2}\int_0^1 dx \int_0^{1-x} dy \frac{x(x-1)}{\Delta}, \tag{B35}$$

where the integrand denominator is common for all $A_3 \ldots A_6$ and reads:

$$\Delta \equiv x(x-1)k_2^2 + y(y-1)k_1^2 - 2xyk_1 \cdot k_2 + m^2. \tag{B36}$$

To estimate the two divergent integrals, A_1 and A_2, we apply the Ward Identities for the vertices ν and ρ, i.e., Eqs. (B27) and (B28) in the expansion (B32) and obtain,

$$\begin{aligned} A_1(k_1, k_2; w) = (k_1 \cdot k_2)A_3(k_1, k_2) + k_1^2 A_4(k_1, k_2) \\ - \frac{m^2 e^3 \beta}{\pi^2} I_1(k_1, k_2, m) \\ + \frac{e^3(\beta^3 + 3\alpha^2\beta)}{4\pi^2}(w-1), \end{aligned} \tag{B37}$$

and,

$$\begin{aligned} A_2(k_1, k_2; z) = (k_1 \cdot k_2)A_6(k_1, k_2) + k_2^2 A_5(k_1, k_2) \\ - \frac{m^2 e^3 \beta}{\pi^2} I_2(k_1, k_2, m) \\ + \frac{e^3(\beta^3 + 3\alpha^2\beta)}{4\pi^2}(z+1). \end{aligned} \tag{B38}$$

Eqs. (B22), (B23), and (B33)–(B38) *complete* the evaluation of the vertex $\Gamma^{\mu\nu\rho}(k_1, k_2, w, z)$ in Eq. (B32). In Appendix D we present analytical expressions of the integrals $A_{3\ldots6}$ and $I_{0,1,2}$ in various limits.

Even if the form factors $A_{i=1\ldots6}$ had not been calculated explicitly there is much to say about their structure by exploiting possible Bose symmetries. Hence, referring to the notation of Fig. 1, Bose symmetry among j and k legs implies,

$$A_1(k_1, k_2) = -A_2(k_2, k_1), \tag{B39a}$$
$$A_3(k_1, k_2) = -A_6(k_2, k_1), \tag{B39b}$$
$$A_4(k_1, k_2) = -A_5(k_2, k_1), \tag{B39c}$$

while in i and j legs,

$$\begin{aligned} A_1(k_1, k_2) = -A_1(-q, k_2) + A_2(-q, k_2) \\ - (k_1 \cdot k_2)[(A_3(-q, k_2) - A_4(-q, k_2)] \\ + k_1^2 A_4(-q, k_2), \end{aligned} \tag{B40a}$$
$$\begin{aligned} A_2(k_1, k_2) = A_2(-q, k_2) + k_2^2[A_3(-q, k_2) \\ - A_4(-q, k_2)] - (k_1 \cdot k_2)A_4(-q, k_2), \end{aligned} \tag{B40b}$$
$$A_3(k_1, k_2) = A_4(-q, k_2) - A_3(-q, k_2), \tag{B40c}$$
$$A_4(k_1, k_2) = A_4(-q, k_2), \tag{B40d}$$
$$\begin{aligned} A_5(k_1, k_2) = A_5(-q, k_2) - A_6(-q, k_2) \\ + A_3(-q, k_2) - A_4(-q, k_2), \end{aligned} \tag{B40e}$$
$$A_6(k_1, k_2) = -A_4(-q, k_2) - A_6(-q, k_2), \tag{B40f}$$

and, finally, in i and k legs we find,

$$\begin{aligned} A_1(k_1, k_2) = A_1(k_{1,} - q) - k_1^2[(A_5(k_1, -q) \\ - A_6(k_1, -q)] - (k_1 \cdot k_2)A_5(k_1, -q), \end{aligned} \tag{B41a}$$
$$\begin{aligned} A_2(k_1, k_2) = A_1(k_1, -q) - A_2(k_1, -q) \\ + (k_1 \cdot k_2)[A_5(k_1, -q) - A_6(k_1, -q)] \\ + k_2^2 A_5(k_1, -q), \end{aligned} \tag{B41b}$$
$$A_3(k_1, k_2) = -A_3(k_1, -q) - A_5(k_1, -q), \tag{B41c}$$
$$\begin{aligned} A_4(k_1, k_2) = A_4(k_1, -q) - A_3(k_1, -q) \\ - A_5(k_1, -q) + A_6(k_1, -q), \end{aligned} \tag{B41d}$$
$$A_5(k_1, k_2) = A_5(k_1, -q), \tag{B41e}$$
$$A_6(k_1, k_2) = A_5(k_1, -q) - A_6(k_1, -q). \tag{B41f}$$

The above relations have been repeatedly used in Sec. IV when determining the anomaly parameters w and z. The reader should notice that in addition to relations due to Bose symmetry, there are few more relations originated solely from fermionic triangle:

$$A_3(k_1, k_2) = A_3(k_2, k_1), \qquad A_6(k_1, k_2) = A_6(k_2, k_1). \tag{B42}$$

We can now exploit Bose symmetry to set constraints on the arbitrary parameters w and z. For example, if the gauge bosons associated with legs j and k in Fig. 1 are identical then Eq. (B39) impose the following relation,

$$w + z = 0, \tag{B43}$$

among the undefined (momentum route dependent) parameters. One last remark is that we can rediscover Bose symmetries by using one of the following equivalent representations (i.e., they leave the double integral measure invariant) of the integrals $A_3 \ldots A_6$ by noting that

$$\Delta(k_1, k_2) \overset{x \leftrightarrow y}{\rightarrow} \Delta(k_2, k_1), \tag{B44}$$

$$\Delta(k_1, k_2) \underset{x \to x}{\overset{y \to 1-x-y}{\rightarrow}} \Delta(k_1, -q), \tag{B45}$$

$$\Delta(k_1, k_2) \underset{x \to 1-x-y}{\overset{y \to y}{\rightarrow}} \Delta(-q, k_2), \tag{B46}$$

where $\Delta(k_1, k_2)$ is a function defined in Eq. (B36).

As a generalization of Eqs. (B15), (B16), and (B18) we can proceed to the situation where there are three, in general different, external gauge bosons with different couplings to fermions. As in (B1), we write the general three point vertex in Fig. 1 as:

$$\Gamma^{\mu\nu\rho}(k_1,k_2;a,b)=\tilde{\Gamma}^{\nu\rho\mu}(k_1,k_2;a,b)=\hat{\Gamma}^{\rho\mu\nu}(k_1,k_2;a,b)=-e^3\int\frac{d^4p}{(2\pi)^4}$$
$$\times\,\mathrm{Tr}\bigg\{\frac{\gamma^\mu(\alpha_i+\beta_i\gamma^5)(\not p-\not k_2+\not a+m)\gamma^\rho(\alpha_j+\beta_j\gamma^5)(\not p+\not a+m)\gamma^\nu(\alpha_k+\beta_k\gamma^5)(\not p+\not k_1+\not a+m)}{[(p-k_2+a)^2-m^2][(p+a)^2-m^2][(p+k_1+a)^2-m^2]}$$
$$+\frac{\gamma^\mu(\alpha_i+\beta_i\gamma^5)(\not p-\not k_1+\not b+m)\gamma^\nu(\alpha_k+\beta_k\gamma^5)(\not p+\not b+m)\gamma^\rho(\alpha_j+\beta_j\gamma^5)(\not p+\not k_2+\not b+m)}{[(p-k_1+b)^2-m^2][(p+b)^2-m^2][(p+k_2+b)^2-m^2]}\bigg\},\tag{B47}$$

and the corresponding two point vertex functions as:

$$\begin{aligned}\Gamma^{\nu\rho}(k_1,k_2)&=\frac{-ie^2m\tilde{\beta}}{2\pi^2}\varepsilon^{\lambda\nu\rho\sigma}k_{1\lambda}k_{2\sigma}\int_0^1dx\int_0^{1-x}dy\frac{(\alpha_j\alpha_k-\beta_j\beta_k)+2\beta_j\beta_k(x+y)}{\Delta},\\ \tilde{\Gamma}^{\rho\mu}(k_1,k_2)&=\frac{ie^2m\tilde{\beta}}{2\pi^2}\varepsilon^{\lambda\mu\xi\rho}k_{1\lambda}k_{2\xi}\int_0^1dx\int_0^{1-x}dy\frac{-(\alpha_i\alpha_k+\beta_i\beta_k)+2x\beta_i\beta_k}{\Delta},\\ \hat{\Gamma}^{\mu\nu}(k_1,k_2)&=\frac{ie^2m\tilde{\beta}}{2\pi^2}\varepsilon^{\lambda\mu\xi\nu}k_{1\lambda}k_{2\xi}\int_0^1dx\int_0^{1-x}dy\frac{(\alpha_i\alpha_j+\beta_i\beta_j)-2y\beta_i\beta_j}{\Delta},\end{aligned}\tag{B48}$$

where as before $\Delta\equiv\Delta(k_1,k_2)$ is given by Eq. (B38). The complete $\Gamma^{\mu\nu\rho}(k_1,k_2,w,z)$ in this general case is presented in section II.

APPENDIX C: CHARGED GAUGE BOSON VERTEX

The calculation for $V^*W^-W^+$, $V=\gamma$, Z is slightly more complicated than the one for neutral triple gauge boson vertices for two reasons: first, the appearance in the loop of two, in general, different fermion masses and second, the appearance of different $Vf\bar{f}$ vertex for each particle contribution (see Fig. 8). Although the first complication leads to only technical difficulties the latter one is more serious: it does not allow for an obvious exploitation of the master 4D "momentum shift" Eq. (B11).

Our method for calculating this vertex follows exactly the same steps as described in detail in Appendix B and in Sec. II. The chiral part of the V^*WW vertex is still given by Eq. (2). The finite form factors $A_3\ldots A_6$ for the first diagram in Fig. 8 are exactly the half of the corresponding ones in (8) but with the replacement of $\Delta(k_1,k_2)$ into

$$\begin{aligned}\Delta(k_1,k_2;m_{f_u}^2,m_{f_d}^2)\equiv{}&x(x-1)k_2^2+y(y-1)k_1^2\\&-2xyk_1\cdot k_2-(x+y)\Delta m^2\\&+m_{f_u}^2,\end{aligned}\tag{C1}$$

with the mass squared difference being $\Delta m^2\equiv m_{f_u}^2-m_{f_d}^2$. f_u and f_d here denote each of the fermion pair (u,ν) and (d,e) for leptons and quarks, respectively. Obviously, the contribution of the crossed diagram i.e., the second diagram in Fig. 8, requires the replacement, $f_u\leftrightarrow f_d$. Our calculation here is quite general and is not confined only in to V^*WW vertex. For example, it could be used for the vertex VW_LW_R in an $SU(2)_L\times SU(2)_R\times U(1)$ gauge model.

As before, the "infinite" form factors, $A_{1,2}$ are fixed by the Ward Identities. The calculation of the first diagram of Fig. 8 results in,

$$\begin{aligned}A_1(k_1,k_2)={}&(k_1\cdot k_2)A_3+k_1^2A_4-\frac{\alpha_j(m_{f_u}-m_{f_d})}{4\pi^2}\\&\times I_{11}(m_{f_u}^2,m_{f_d}^2)-\frac{\beta_j(m_{f_u}+m_{f_d})}{4\pi^2}\\&\times I_{12}(m_{f_u}^2,m_{f_d}^2)+\frac{c}{8\pi^2}(w-1),\end{aligned}\tag{C2a}$$

$$\begin{aligned}A_2(k_1,k_2)={}&(k_1\cdot k_2)A_6+k_2^2A_5+\frac{\alpha_k(m_{f_u}-m_{f_d})}{4\pi^2}\\&\times I_{21}(m_{f_u}^2,m_{f_d}^2)-\frac{\beta_k(m_{f_u}+m_{f_d})}{4\pi^2}\\&\times I_{22}(m_{f_u}^2,m_{f_d}^2)+\frac{c}{8\pi^2}(z+1),\end{aligned}\tag{C2b}$$

where $c\equiv(\alpha_i\alpha_j+\beta_i\beta_j)\beta_k+(\alpha_i\beta_j+\alpha_j\beta_i)\alpha_k$ is the usual anomaly factor. Again, the result depends upon two arbitrary four vectors, a^μ and b^μ, that parameterize the momentum routing in the loop. For chiral gauge anomalies to cancel after summing over all fermions, the arbitrary

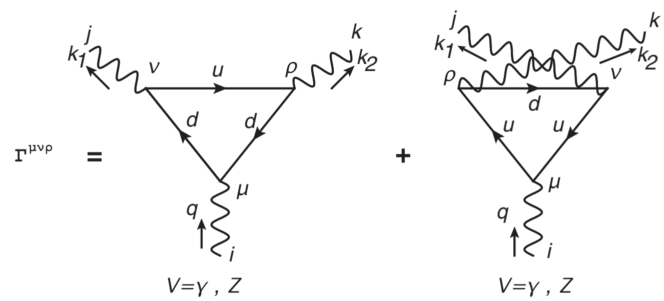

FIG. 8. The one-loop effective triple gauge boson vertex, $\Gamma^{\mu\nu\rho}_{VW^-W^+}$, $V=\gamma$, Z. As in Fig. 1, indices $\{i,j,k\}$ denote distinct external gauge bosons in general.

vectors a^μ and b^μ need to be set at $a^\mu = -b^\mu$. As before, we write a^μ as a linear combination of independent four vectors as $a^\mu = zk_1^\mu + wk_2^\mu$, with z, w arbitrary real parameters. This includes γ, Z, W-self energy corrections. The latter depend on their own routing momenta arbitrary vectors that can be taken as such in order to eliminate their anomalous contributions. One then expects that this relation renders the nonchiral part independent of a^μ as it does for the neutral vertices VVV, for $V = \gamma$, Z [see Appendix B]. However, for VWW-vertices there are additional contributions to the nonchiral part of $\Gamma^{\mu\nu\rho}$ from Z, γ, W-self energy corrections that depend on routing momentum arbitrary vectors. When all these corrections are added one expects the result to be independent on these arbitrary vectors.

Then the "nondecoupling" integrals, $I_{ij} \equiv I_{ij}(m_{f_u}^2, m_{f_d}^2)$ with i, $j = 1, 2$, appearing in Eq. (C2) are given by

$$I_{11} = \int_0^1 dx \int_0^{1-x} dy \frac{(\alpha_i\beta_k + \alpha_k\beta_i)m_{f_d}y + (\alpha_i\beta_k + \alpha_k\beta_i)m_{f_u}(x+y-1) + (\alpha_i\beta_k - \alpha_k\beta_i)m_{f_d}x}{\Delta(k_1, k_2; m_{f_u}^2, m_{f_d}^2)}, \tag{C3a}$$

$$I_{12} = \int_0^1 dx \int_0^{1-x} dy \frac{-(\alpha_i\alpha_k + \beta_i\beta_k)m_{f_d}y + (\alpha_i\alpha_k + \beta_i\beta_k)m_{f_u}(x+y-1) - (\alpha_i\alpha_k - \beta_i\beta_k)m_{f_d}x}{\Delta(k_1, k_2; m_{f_u}^2, m_{f_d}^2)}, \tag{C3b}$$

$$I_{21} = \int_0^1 dx \int_0^{1-x} dy \frac{(\alpha_i\beta_j - \alpha_j\beta_i)m_{f_d}y + (\alpha_i\beta_j + \alpha_j\beta_i)m_{f_u}(x+y-1) + (\alpha_i\beta_j + \alpha_j\beta_i)m_{f_d}x}{\Delta(k_1, k_2; m_{f_u}^2, m_{f_d}^2)}, \tag{C3c}$$

$$I_{22} = \int_0^1 dx \int_0^{1-x} dy \frac{(\alpha_i\alpha_j - \beta_i\beta_j)m_{f_d}y - (\alpha_i\alpha_j + \beta_i\beta_j)m_{f_u}(x+y-1) + (\alpha_i\alpha_j + \beta_i\beta_j)m_{f_d}x}{\Delta(k_1, k_2; m_{f_u}^2, m_{f_d}^2)}, \tag{C3d}$$

where $\alpha_i \equiv \alpha_{f_d}$, $\beta_i \equiv \beta_{f_d}, \ldots$ etc, follow the first diagram of Fig. 8. The corresponding expressions for the crossed diagram are easily obtained from those in Eqs. (C2) and (C3) with the replacement $f_u \leftrightarrow f_d$. Note that CP-invariance is maintained since $A_1(k_1, k_2) = -A_2(k_2, k_1)$.

For reasons we explained at the beginning of this Appendix, finding the anomalous terms i.e., the last terms in Eq. (C2), is not a straightforward task. The trick here is to add a Lorentz invariant but vanishing integral that generates exactly the anomaly integrals by momentum shift. It is then straightforward to use the 4-D expression (B11).

To complete our analysis for the chiral fermionic triangle with general external charged and neutral gauge bosons, we append here the relevant WI's analogous to those presented in Eq. (3) for neutral external gauge bosons:

$$q_\mu\Gamma^{\mu\nu\rho}(k_1, k_2) = -\frac{\beta_i}{2\pi^2} m_{f_d}\epsilon^{\nu\rho\lambda\sigma}k_{1\lambda}k_{2\sigma}I_{01}(m_{f_u}^2, m_{f_d}^2) + \frac{c}{8\pi^2}\epsilon^{\nu\rho\lambda\sigma}k_{1\lambda}k_{2\sigma}(w - z), \tag{C4a}$$

$$\begin{aligned}-k_{1\nu}\Gamma^{\mu\nu\rho}(k_1, k_2) = {}& -\frac{\alpha_j}{4\pi^2}(m_{f_u} - m_{f_d})\epsilon^{\mu\rho\lambda\sigma}k_{1\lambda}k_{2\sigma}I_{11}(m_{f_u}^2, m_{f_d}^2) - \frac{\beta_j}{4\pi^2}(m_{f_u} + m_{f_d})\epsilon^{\mu\rho\lambda\sigma}k_{1\lambda}k_{2\sigma}I_{12}(m_{f_u}^2, m_{f_d}^2)\\ & + \frac{c}{8\pi^2}\epsilon^{\mu\rho\lambda\sigma}k_{1\lambda}k_{2\sigma}(w - 1),\end{aligned} \tag{C4b}$$

$$\begin{aligned}-k_{2\rho}\Gamma^{\mu\nu\rho}(k_1, k_2) = {}& \frac{\alpha_k}{4\pi^2}(m_{f_u} - m_{f_d})\epsilon^{\mu\nu\lambda\sigma}k_{1\lambda}k_{2\sigma}I_{21}(m_{f_u}^2, m_{f_d}^2) - \frac{\beta_k}{4\pi^2}(m_{f_u} + m_{f_d})\epsilon^{\mu\nu\lambda\sigma}k_{1\lambda}k_{2\sigma}I_{22}(m_{f_u}^2, m_{f_d}^2)\\ & + \frac{c}{8\pi^2}\epsilon^{\mu\nu\lambda\sigma}k_{1\lambda}k_{2\sigma}(z + 1).\end{aligned} \tag{C4c}$$

Again, the corresponding expressions for the crossed diagram in Fig. 8 are obtained from Eq. (C4) after the replacement $f_u \leftrightarrow f_d$. The integral $I_{01} \equiv I_{01}(m_{f_u}^2, m_{f_d}^2)$ is given by

$$I_{01} = \int_0^1 dx \int_0^{1-x} dy \frac{(\alpha_j\alpha_k + \beta_j\beta_k)m_{f_d}y - (\alpha_j\alpha_k - \beta_j\beta_k)m_{f_u}(x+y-1) + (\alpha_j\alpha_k + \beta_j\beta_k)m_{f_d}x}{\Delta(k_1, k_2; m_{f_u}^2, m_{f_d}^2)}. \tag{C5}$$

As a check, note that in the limit of equal masses $m_{f_u}^2 = m_{f_d}^2$ all the above integral expressions reduce to the corresponding ones in Eqs. (4), (5), and (8) for the neural gauge boson vertex.

APPENDIX D: SOME USEFUL ANALYTICAL INTEGRAL EXPRESSIONS

In this Appendix we present analytical expressions for integrals related to $A_{3\ldots6}$, and, $I_{1,2}$ in the limit where $k_1^2, k_2^2 \to 0$ as well as their approximate expressions in various limits. We make an effort to write the latter in terms of standard functions i.e., *not* dilogarithms, which are easy to handle both symbolically and numerically. We start out with integrals related to Eq. (8),

$$\tilde{A}_3(\xi) = \int_0^1 dx \int_0^{1-x} dy \frac{xy}{xy - \xi/4} = \frac{1}{2}[1 + \xi J(\xi)], \tag{D1}$$

where $\xi \equiv \frac{4m^2}{s}$, m is the loop fermion mass, and $s = (k_1 + k_2)^2$, while,

$$J(\xi) = -\arctan^2\left(\frac{1}{\sqrt{\xi - 1}}\right), \qquad \xi \geq 1, \tag{D2a}$$

$$= \frac{1}{4}\left[\ln\left(\frac{1 - \sqrt{1-\xi}}{1 + \sqrt{1-\xi}}\right) - i\pi\right]^2, \qquad \xi \leq 1. \tag{D2b}$$

This integral has also been calculated in Ref. [62] and we find agreement. In the same limit the integral related to A_4 and A_5 is:

$$\tilde{A}_4(\xi) = \tilde{A}_5(\xi) = \int_0^1 dx \int_0^{1-x} dy \frac{x(x-1)}{xy - \xi/4} = \int_0^1 dx \int_0^{1-x} dy \frac{y(y-1)}{xy - \xi/4}, \tag{D3}$$

with its exact answer written like

$$\tilde{A}_4(\xi) = 1 - \sqrt{\xi - 1}\arctan\left(\frac{1}{\sqrt{\xi - 1}}\right), \qquad \xi \geq 1, \tag{D4}$$

$$= 1 + \frac{\sqrt{1-\xi}}{2}\left[\ln\left(\frac{1 - \sqrt{1-\xi}}{1 + \sqrt{1-\xi}}\right) - i\pi\right], \qquad \xi \leq 1. \tag{D5}$$

Integrals that are related to I_1 and I_2 of Eq. (5) are:

$$\tilde{I}_1(\xi) = \int_0^1 dx \int_0^{1-x} dy \frac{1}{xy - \xi/4} \tag{D6}$$

$$= -2\arctan^2\left(\frac{1}{\sqrt{\xi - 1}}\right), \qquad \xi \geq 1 \tag{D7}$$

$$= \frac{1}{2}\left[\ln\left(\frac{1 - \sqrt{1-\xi}}{1 + \sqrt{1-\xi}}\right) - i\pi\right]^2, \qquad \xi \leq 1, \tag{D8}$$

and

$$\tilde{I}_1'(\xi) = \int_0^1 dx \int_0^{1-x} dy \frac{x}{xy - \xi/4} = \int_0^1 dx \int_0^{1-x} dy \frac{y}{xy - \xi/4} \tag{D9}$$

$$= 2\left[\sqrt{\xi - 1}\arctan\left(\frac{1}{\sqrt{\xi - 1}}\right) - 1\right], \qquad \xi \geq 1 \tag{D10}$$

$$= -2 - \sqrt{1-\xi}\left[\ln\left(\frac{1 - \sqrt{1-\xi}}{1 + \sqrt{1-\xi}}\right) - i\pi\right], \qquad \xi \leq 1. \tag{D11}$$

These integrals are related to standard ones, $A_3 \ldots A_6$, $I_{1,2}$, and in the limit where $m_Z^2 \ll s < m^2$, become

$$A_3(s;m^2) = -A_6(s;m^2) = \frac{c}{s}\tilde{A}_3\left(\frac{4m^2}{s}\right) = -\frac{c}{m^2}\left[\frac{1}{24} + \frac{1}{180}\frac{s}{m^2} + O(s^2/m^4)\right], \tag{D12a}$$

$$A_4(s;m^2) = -A_5(s;m^2) = -\frac{c}{s}\tilde{A}_4\left(\frac{4m^2}{s}\right) = -\frac{c}{m^2}\left[\frac{1}{12} + \frac{1}{120}\frac{s}{m^2} + O(s^2/m^4)\right], \tag{D12b}$$

$$I_1(s;m^2) = \frac{\alpha_i\alpha_k + \beta_i\beta_k}{s}\tilde{I}_1\left(\frac{4m^2}{s}\right) - \frac{2\beta_i\beta_k}{s}\tilde{I}_1'\left(\frac{4m^2}{s}\right) = -\frac{1}{m^2}\left[\frac{\beta_i\beta_k + 3\alpha_i\alpha_k}{6} + \frac{\beta_i\beta_k + 5\alpha_i\alpha_k}{120}\frac{s}{m^2} + O(s^2/m^4)\right], \tag{D12c}$$

$$I_2(s;m^2) = -\frac{\alpha_i\alpha_j + \beta_i\beta_j}{s}\tilde{I}_1\left(\frac{4m^2}{s}\right) + \frac{2\beta_i\beta_j}{s}\tilde{I}_1'\left(\frac{4m^2}{s}\right) = \frac{1}{m^2}\left[\frac{\beta_i\beta_j + 3\alpha_i\alpha_j}{6} + \frac{\beta_i\beta_j + 5\alpha_i\alpha_j}{120}\frac{s}{m^2} + O(s^2/m^4)\right], \tag{D12d}$$

where $c = \frac{e^3[(\alpha_i\alpha_j+\beta_i\beta_j)\beta_k+(\alpha_i\beta_j+\beta_i\alpha_j)\alpha_k]}{\pi^2}$ is the anomaly factor. These expressions are in agreement with the corresponding ones presented in Ref. [5]. In the high energy limit $m^2 \ll s$, we obtain,

$$A_3(s;m^2) = -A_6(s;m^2) \simeq c\left\{\frac{1}{2s} + \frac{m^2}{2s^2}\left[\ln^2\frac{s}{m^2} - \pi^2\right] + i\pi\frac{m^2}{s^2}\ln\frac{s}{m^2} + O(m^4/s^3)\right\}, \tag{D13a}$$

$$A_4(s;m^2) = -A_5(s;m^2) \simeq c\left\{\frac{1}{s}\left[-1 + \frac{1}{2}\ln\frac{s}{m^2}\right] - \frac{m^2}{s^2}\left[\ln\frac{s}{m^2} + 1\right] + i\pi\left[\frac{1}{2s} - \frac{m^2}{s^2}\right] + O(m^4/s^3)\right\}, \tag{D13b}$$

$$\begin{aligned} I_1(s;m^2) \simeq{}& \frac{(\alpha_i\alpha_k + \beta_i\beta_k)}{s}\left[\frac{1}{2}\left(\ln^2\frac{s}{m^2} - \pi^2\right) - 2\frac{m^2}{s}\ln\frac{s}{m^2}\right] - \frac{2\beta_i\beta_k}{s}\left[\ln\frac{s}{m^2} - 2 - \frac{2m^2}{s}\left(\ln\frac{s}{m^2} + 1\right)\right] \\ &+ i\pi\left\{\frac{(\alpha_i\alpha_k + \beta_i\beta_k)}{s}\left[\ln\frac{s}{m^2} - \frac{2m^2}{s}\right] - \frac{2\beta_i\beta_k}{s}\left[1 - \frac{2m^2}{s}\right]\right\} + O(m^4/s^3), \end{aligned} \tag{D13c}$$

$$\begin{aligned} I_2(s;m^2) \simeq{}& -\frac{(\alpha_i\alpha_j + \beta_i\beta_j)}{s}\left[\frac{1}{2}\left(\ln^2\frac{s}{m^2} - \pi^2\right) - 2\frac{m^2}{s}\ln\frac{s}{m^2}\right] + \frac{2\beta_i\beta_j}{s}\left[\ln\frac{s}{m^2} - 2 - \frac{2m^2}{s}\left(\ln\frac{s}{m^2} + 1\right)\right] \\ &- i\pi\left\{\frac{(\alpha_i\alpha_j + \beta_i\beta_j)}{s}\left[\ln\frac{s}{m^2} - \frac{2m^2}{s}\right] - \frac{2\beta_i\beta_j}{s}\left[1 - \frac{2m^2}{s}\right]\right\} + O(m^4/s^3). \end{aligned} \tag{D13d}$$

Only the real parts of these expressions have been presented in Ref. [5] and we find agreement.[12] Other useful identities among A's that have been used in our numerical code for calculating the V^*ZZ-vertex are,

$$(A_3 - A_4)(k_1 = m_Z, k_2 = m_Z, s; m = 0) = -\frac{1}{4m_Z^2} + \frac{s}{2m_Z^2}A_3(k_1 = m_Z, k_2 = m_Z, s; m = 0), \tag{D14}$$

and for the $V^*\gamma Z$-vertex,

$$A_3(k_1 = 0, k_2 = m_Z, s; m = 0) = \frac{1}{2(s - m_Z^2)} - \frac{m_Z^2}{2(s - m_Z^2)^2}\ln\left(\frac{s}{m_Z^2}\right), \tag{D15}$$

$$A_5(k_1 = 0, k_2 = m_Z, s; m = 0) = -\frac{1}{2(s - m_Z^2)}\ln\left(\frac{s}{m_Z^2}\right). \tag{D16}$$

Finally, we derive full analytical expressions in the case $k_1^2 = 0$, where one of the external gauge bosons is massless e.g., the $V^*\gamma Z$-vertex. To this end it is useful to define an auxiliary function,

$$\mathcal{F}(m_Z, s, m) \equiv \int_0^1 dx \int_0^{1-x} dy \ln[x(x-1)m_Z^2 - xy(s - m_Z^2) + m^2], \tag{D17}$$

out of which we read $A_3 \ldots A_6$, $I_{1,2}$ by simply taking appropriate derivatives w.r.t s, $k_2^2 = m_Z^2$ or m^2. Depending on the region of parameters s, m^2, m_Z^2 we have found the function $\mathcal{F}$ to be,

$$\begin{aligned} \mathcal{F}(m_Z, s, m) ={}& -\frac{3}{2} + \frac{\ln(m^2)}{2} - \left(\frac{1}{m_Z^2 - s}\right)\left\{s\sqrt{\frac{4m^2}{s} - 1}\arctan\left(\frac{1}{\sqrt{\frac{4m^2}{s} - 1}}\right) - m_Z^2\sqrt{\frac{4m^2}{m_Z^2} - 1}\arctan\left(\frac{1}{\sqrt{\frac{4m^2}{m_Z^2} - 1}}\right)\right. \\ &\left. + 2m^2\left[\arctan^2\left(\frac{1}{\sqrt{\frac{4m^2}{s} - 1}}\right) - \arctan^2\left(\frac{1}{\sqrt{\frac{4m^2}{m_Z^2} - 1}}\right)\right]\right\}, \qquad \frac{4m^2}{s} > 1, \qquad \frac{4m^2}{m_Z^2} > 1, \end{aligned} \tag{D18}$$

[12] For notational matter, our integrals are related to those in Ref. [5] like $A_3 = -c_6$, $A_4 = \frac{1}{2}(c_4 - c_3 - 2c_6)$, where for example $A_3 \equiv A_3(k_1^2 = k_2^2 = m_W^2, s, m_{f_u}^2, m_{f_d}^2), \ldots$ etc.

$$\mathcal{F}(m_Z,s,m)=-\frac{3}{2}+\frac{\ln(m^2)}{2}-\left(\frac{1}{m_Z^2-s}\right)\left\{s\sqrt{\frac{4m^2}{s}-1}\arctan\left(\frac{1}{\sqrt{\frac{4m^2}{s}-1}}\right)+m_Z^2\left[\frac{1}{2}\sqrt{1-\frac{4m^2}{m_Z^2}}\left(\ln\left(\frac{1-\sqrt{1-\frac{4m^2}{m_Z^2}}}{1+\sqrt{1-\frac{4m^2}{m_Z^2}}}\right)-i\pi\right)\right]\right.$$
$$\left.+m^2\left[2\arctan^2\left(\frac{1}{\sqrt{\frac{4m^2}{s}-1}}\right)+\frac{1}{2}\left(\ln\left(\frac{1-\sqrt{1-\frac{4m^2}{m_Z^2}}}{1+\sqrt{1-\frac{4m^2}{m_Z^2}}}\right)+i\pi\right)^2\right]\right\},\qquad \frac{4m^2}{s}>1,\qquad \frac{4m^2}{m_Z^2}<1, \tag{D19}$$

$$\mathcal{F}(m_Z,s,m)=-\frac{3}{2}+\frac{\ln(m^2)}{2}+\left(\frac{1}{m_Z^2-s}\right)\left\{s\left[\frac{1}{2}\sqrt{1-\frac{4m^2}{s}}\left(\ln\left(\frac{1-\sqrt{1-\frac{4m^2}{s}}}{1+\sqrt{1-\frac{4m^2}{s}}}\right)-i\pi\right)\right]+m_Z^2\left[\sqrt{\frac{4m^2}{m_Z^2}-1}\arctan\left(\frac{1}{\sqrt{\frac{4m^2}{m_Z^2}-1}}\right)\right]\right.$$
$$\left.+m^2\left[2\arctan^2\left(\frac{1}{\sqrt{\frac{4m^2}{m_Z^2}-1}}\right)+\frac{1}{2}\left(\ln\left(\frac{1-\sqrt{1-\frac{4m^2}{s}}}{1+\sqrt{1-\frac{4m^2}{s}}}\right)-i\pi\right)^2\right]\right\},\qquad \frac{4m^2}{s}<1,\qquad \frac{4m^2}{m_Z^2}>1, \tag{D20}$$

$$\mathcal{F}(m_Z,s,m)=-\frac{3}{2}+\frac{\ln(m^2)}{2}+\left(\frac{1}{m_Z^2-s}\right)\left\{s\left[\frac{1}{2}\sqrt{1-\frac{4m^2}{s}}\left(\ln\left(\frac{1-\sqrt{1-\frac{4m^2}{s}}}{1+\sqrt{1-\frac{4m^2}{s}}}\right)-i\pi\right)\right]\right.$$
$$-m_Z^2\left[\frac{1}{2}\sqrt{1-\frac{4m^2}{m_Z^2}}\left(\ln\left(\frac{1-\sqrt{1-\frac{4m^2}{m_Z^2}}}{1+\sqrt{1-\frac{4m^2}{m_Z^2}}}\right)-i\pi\right)\right]+m^2\left[\frac{1}{2}\left(\ln\left(\frac{1-\sqrt{1-\frac{4m^2}{s}}}{1+\sqrt{1-\frac{4m^2}{s}}}\right)\pm i\pi\right)^2\right.$$
$$\left.\left.-\frac{1}{2}\left(\ln\left(\frac{1-\sqrt{1-\frac{4m^2}{m_Z^2}}}{1+\sqrt{1-\frac{4m^2}{m_Z^2}}}\right)\pm i\pi\right)^2\right]\right\},\qquad \frac{4m^2}{s}<1,\qquad \frac{4m^2}{m_Z^2}<1. \tag{D21}$$

In Eq. (D21), the plus sign corresponds to $s<m_Z^2$ while the minus sign to $s>m_Z^2$. As an example the full analytical expressions for A_3 and A_5 can be obtained by taking appropriate derivatives of function $\mathcal{F}$ like, $A_3=c\frac{\partial\mathcal{F}}{\partial s}$ and $A_5=-c\left(\frac{\partial\mathcal{F}}{\partial s}+\frac{\partial\mathcal{F}}{\partial m_Z^2}\right)$, where, as above, c is a factor related to the couplings in the corresponding vertex. As a cross check, taking the limit $m\longrightarrow 0$ in Eq. (D21) we arrive at,

$$F(m_Z,s,0)=-\frac{3}{2}-\frac{1}{2(m_Z^2-s)}[s\ln(s)-m_Z^2\ln(m_Z^2)]+\frac{i\pi}{2}, \tag{D22}$$

and differentiating w.r.t s and m_Z^2 we reproduce the expressions Eqs. (D15) and (D16).

APPENDIX E: CONDITIONS FOR NONDECOUPLING EFFECTS IN X, Y, Z MODEL

In this appendix we present necessary conditions for anomaly cancellation and nondecoupling heavy fermion effects in a model with three different $U(1)$'s corresponding to three distinct massive or massless gauge bosons X, Y, and Z. For this model to be anomaly-free, the following conditions among couplings [see Eq. (1)]:

$$\sum_{i=1}^{n}(\beta_X^3 + 3\alpha_X^2\beta_X)_i = \sum_{i=1}^{n}(\beta_Y^3 + 3\alpha_Y^2\beta_Y)_i = \sum_{i=1}^{n}(\beta_Z^3 + 3\alpha_Z^2\beta_Z)_i = 0,$$
$$\sum_{i=1}^{n}(\beta_X^2\beta_Y + 2\alpha_X\alpha_Y\beta_X + \alpha_X^2\beta_Y)_i = \sum_{i=1}^{n}(\beta_X^2\beta_Z + 2\alpha_X\alpha_Z\beta_X + \alpha_X^2\beta_Z)_i = \sum_{i=1}^{n}(\beta_Y^2\beta_X + 2\alpha_X\alpha_Y\beta_Y + \alpha_Y^2\beta_X)_i = 0,$$
$$\sum_{i=1}^{n}(\beta_Y^2\beta_Z + 2\alpha_Z\alpha_Y\beta_Y + \alpha_Y^2\beta_Z)_i = \sum_{i=1}^{n}(\beta_Z^2\beta_X + 2\alpha_X\alpha_Z\beta_Z + \alpha_Z^2\beta_X)_i = \sum_{i=1}^{n}(\beta_Z^2\beta_Y + 2\alpha_Z\alpha_Y\beta_Z + \alpha_Z^2\beta_Y)_i = 0,$$
$$\sum_{i=1}^{n}(\beta_X\beta_Y\beta_Z + \alpha_X\alpha_Z\beta_Y + \alpha_X\alpha_Y\beta_Z + \alpha_Z\alpha_Y\beta_X)_i = 0, \tag{E1}$$

must hold. Nondecoupling effects in XYZ-vertex are activated if, in addition to the requirements in Eq. (E1), at least one of the following expressions is nonzero:

$$\sum_{i=1}^{n}(\beta_X^2\beta_Y + 3\alpha_X\alpha_Y\beta_X)_i, \quad \sum_{i=1}^{n}(\beta_X^2\beta_Y + 3\alpha_X^2\beta_Y)_i, \quad \sum_{i=1}^{n}(\beta_X^2\beta_Z + 3\alpha_X\alpha_Z\beta_X)_i, \quad \sum_{i=1}^{n}(\beta_X^2\beta_Z + 3\alpha_X^2\beta_Z)_i,$$
$$\sum_{i=1}^{n}(\beta_Y^2\beta_X + 3\alpha_X\alpha_Y\beta_Y)_i \quad \sum_{i=1}^{n}(\beta_Y^2\beta_X + 3\alpha_Y^2\beta_X)_i, \quad \sum_{i=1}^{n}(\beta_Y^2\beta_Z + 3\alpha_Y\alpha_Z\beta_Y)_i, \quad \sum_{i=1}^{n}(\beta_Y^2\beta_Z + 3\alpha_Y^2\beta_Z)_i,$$
$$\sum_{i=1}^{n}(\beta_Z^2\beta_X + 3\alpha_X\alpha_Z\beta_Z)_i \quad \sum_{i=1}^{n}(\beta_Z^2\beta_X + 3\alpha_Z^2\beta_X)_i, \quad \sum_{i=1}^{n}(\beta_Z^2\beta_Y + 3\alpha_Y\alpha_Z\beta_Z)_i, \quad \sum_{i=1}^{n}(\beta_Z^2\beta_Y + 3\alpha_Z^2\beta_Y)_i,$$
$$\sum_{i=1}^{n}(\beta_X\beta_Y\beta_Z + 3\alpha_X\alpha_Z\beta_Y)_i \quad \sum_{i=1}^{n}(\beta_X\beta_Y\beta_Z + 3\alpha_X\alpha_Y\beta_Z)_i, \quad \sum_{i=1}^{n}(\beta_X\beta_Y\beta_Z + 3\alpha_Y\alpha_Z\beta_X)_i. \tag{E2}$$

[1] T. Appelquist and J. Carazzone, Phys. Rev. D **11**, 2856 (1975).
[2] S. Glashow, Nucl. Phys. **22**, 579 (1961).
[3] S. Weinberg, Phys. Rev. Lett. **19**, 1264 (1967).
[4] A. Salam, in *Proceedings of the Eighth Nobel Symposium*, edited by N. Svartholm (Wiley, New York, 1968), p. 367.
[5] C.-r. Ahn, M.E. Peskin, B.W. Lynn, and S.B. Selipsky, Nucl. Phys. **B309**, 221 (1988).
[6] D. Kennedy, Phys. Lett. B **268**, 86 (1991).
[7] S.L. Adler, Phys. Rev. **177**, 2426 (1969).
[8] J. Bell and R. Jackiw, Nuovo Cimento A **60**, 47 (1969).
[9] W.A. Bardeen, Phys. Rev. **184**, 1848 (1969).
[10] K. Fujikawa, Phys. Rev. D **21**, 2848 (1980).
[11] J.A. Harvey, arXiv:hep-th/0509097.
[12] C.T. Hill, arXiv:hep-th/0601155.
[13] A. Bilal, arXiv:0802.0634.
[14] C. Bouchiat, J. Iliopoulos, and P. Meyer, Phys. Lett. B **38**, 519 (1972).
[15] D.J. Gross and R. Jackiw, Phys. Rev. D **6**, 477 (1972).
[16] E. D'Hoker and E. Farhi, Nucl. Phys. **B248**, 77 (1984).
[17] E. D'Hoker and E. Farhi, Nucl. Phys. **B248**, 59 (1984).
[18] J. Wess and B. Zumino, Phys. Lett. B **37**, 95 (1971).
[19] E. Witten, Nucl. Phys. **B223**, 422 (1983).
[20] O. Kaymakcalan, S. Rajeev, and J. Schechter, Phys. Rev. D **30**, 594 (1984).
[21] J.A. Harvey, C.T. Hill, and R.J. Hill, Phys. Rev. D **77**, 085017 (2008).
[22] J.A. Harvey, C.T. Hill, and R.J. Hill, Phys. Rev. Lett. **99**, 261601 (2007).
[23] J.L. Diaz-Cruz, Phys. Rev. D **56**, 523 (1997).
[24] E. D'Hoker, Phys. Rev. Lett. **69**, 1316 (1992).
[25] G.-L. Lin, H. Steger, and Y.-P. Yao, Phys. Rev. D **44**, 2139 (1991).
[26] F. Feruglio, A. Masiero, and L. Maiani, Nucl. Phys. **B387**, 523 (1992).
[27] R. Jackiw, Int. J. Mod. Phys. B **14**, 2011 (2000).
[28] I. Antoniadis, A. Boyarsky, S. Espahbodi, O. Ruchayskiy, and J.D. Wells, Nucl. Phys. **B824**, 296 (2010).
[29] E. Dudas, Y. Mambrini, S. Pokorski, and A. Romagnoni, J. High Energy Phys. 08 (2009) 014.
[30] J. Preskill, Ann. Phys. (N.Y.) **210**, 323 (1991).
[31] P. Anastasopoulos, M. Bianchi, E. Dudas, and E. Kiritsis, J. High Energy Phys. 11 (2006) 057.
[32] J. Kumar, A. Rajaraman, and J.D. Wells, Phys. Rev. D **77**, 066011 (2008).
[33] C. Coriano, N. Irges, and S. Morelli, J. High Energy Phys. 07 (2007) 008.
[34] N. Irges, C. Coriano, and S. Morelli, Nucl. Phys. **B789**, 133 (2008).
[35] R. Armillis, C. Coriano, and M. Guzzi, J. High Energy Phys. 05 (2008) 015.
[36] K. Hagiwara, R. Peccei, D. Zeppenfeld, and K. Hikasa, Nucl. Phys. **B282**, 253 (1987).
[37] K. Gaemers and G. Gounaris, Z. Phys. C **1**, 259 (1979).
[38] L. Rosenberg, Phys. Rev. **129**, 2786 (1963).

[39] A. Barroso, F. Boudjema, J. Cole, and N. Dombey, Z. Phys. C **28**, 149 (1985).
[40] U. Baur and E. L. Berger, Phys. Rev. D **47**, 4889 (1993).
[41] G. Gounaris, J. Layssac, and F. Renard, Phys. Rev. D **61**, 073013 (2000).
[42] G. Gounaris, J. Layssac, and F. Renard, Phys. Rev. D **62**, 073013 (2000).
[43] G. Gounaris, J. Layssac, and F. Renard, Phys. Rev. D **62**, 073012 (2000).
[44] A. Dedes, I. Giomataris, K. Suxho, and J. Vergados, Nucl. Phys. **B826**, 148 (2010).
[45] J. Kopp, V. Niro, T. Schwetz, and J. Zupan, Phys. Rev. D **80**, 083502 (2009).
[46] M. Williams, C. Burgess, A. Maharana, and F. Quevedo, J. High Energy Phys. 08 (2011) 106.
[47] G. 't Hooft and M. Veltman, Nucl. Phys. **B44**, 189 (1972).
[48] J. Jauch and F. Rohrlich, *The Theory of Photons and Electrons* (Springer-Verlag, New York, 1976).
[49] R. Pugh, Can. J. Phys. **47**, 1263 (1969).
[50] V. Elias, G. McKeon, and R. B. Mann, Phys. Rev. D **28**, 1978 (1983).
[51] J. M. Cornwall, D. N. Levin, and G. Tiktopoulos, Phys. Rev. D **10**, 1145 (1974).
[52] C. E. Vayonakis, Nuovo Cimento Soc. Ital. Fis. A **17**, 383 (1976).
[53] B. W. Lee, C. Quigg, and H. B. Thacker, Phys. Rev. D **16**, 1519 (1977).
[54] J. Abdallah *et al.* (DELPHI), Eur. Phys. J. C **51**, 525 (2007).
[55] V. M. Abazov *et al.* (D0 Collaboration), Phys. Lett. B **671**, 349 (2009).
[56] T. Aaltonen *et al.* (CDF Collaboration), Phys. Rev. Lett. **107**, 051802 (2011).
[57] P.-F. Giraud, arXiv:1201.4868.
[58] A. Martelli, arXiv:1201.4596.
[59] L. D. Landau, Dokl. Akad. Nauk SSSR **60**, 207 (1948).
[60] C.-N. Yang, Phys. Rev. **77**, 242 (1950).
[61] S. Aminneborg, L. Bergstrom, and B. A. Lindholm, Phys. Rev. D **43**, 2527 (1991).
[62] S. Rudaz, Phys. Rev. D **39**, 3549 (1989).
[63] J. Abdallah *et al.* (The DELPHI Collaboration), Eur. Phys. J. C **66**, 35 (2010).
[64] V. M. Abazov *et al.* (The D0 Collaboration), Phys. Rev. Lett. **107**, 241803 (2011).
[65] M. E. Peskin and T. Takeuchi, Phys. Rev. D **46**, 381 (1992).
[66] M. Baak *et al.*, arXiv:1107.0975.
[67] T. Aaltonen *et al.* (CDF Collaboration), Phys. Rev. Lett. **106**, 141803 (2011).
[68] M. E. Peskin, arXiv:1110.3805.
[69] A. Wingerter, Phys. Rev. D **84**, 095012 (2011).
[70] P. Langacker, Rev. Mod. Phys. **81**, 1199 (2009).
[71] T. Appelquist, B. A. Dobrescu, and A. R. Hopper, Phys. Rev. D **68**, 035012 (2003).
[72] E. Salvioni, G. Villadoro, and F. Zwirner, J. High Energy Phys. 11 (2009) 068.
[73] E. Salvioni, A. Strumia, G. Villadoro, and F. Zwirner, J. High Energy Phys. 03 (2010) 010.
[74] N. Deshpande and J. Trampetic, Phys. Lett. B **206**, 665 (1988).
[75] W.-Y. Keung, I. Low, and J. Shu, Phys. Rev. Lett. **101**, 091802 (2008).
[76] M. E. Peskin and D. V. Schroeder, *Reading* (Addison-Wesley, USA, 1995), p. 842.
[77] S. B. Treiman, E. Witten, R. Jackiw, and B. Zumino, *Current Algebra and Anomalies* (World Scientific, Singapore, 1985), p. 537
[78] S. Weinberg, *The Quantum Theory of Fields, Volume 2: Modern Applications* (Cambridge University Press, Cambridge, 1996), p. 489.
[79] H. K. Dreiner, H. E. Haber, and S. P. Martin, Phys. Rep. **494**, 1 (2010).